Earth Syst. Sci. Data, 15, 1655–1673, 2023
https://doi.org/10.5194/essd-15-1655-2023

Open Access Earth System Science Data

A strontium isoscape of northern Australia

Patrice de Caritat[1], **Anthony Dosseto**[2], **and Florian Dux**[2]

[1]Geoscience Australia, GPO Box 378, Canberra, ACT 2601, Australia
[2]Wollongong Isotope Geochronology Laboratory, School of Earth, Atmospheric and Life Sciences, University of Wollongong, Wollongong, NSW 2522, Australia

Correspondence: Patrice de Caritat (patrice.decaritat@ga.gov.au)

Received: 16 December 2022 – Discussion started: 16 January 2023
Revised: 15 March 2023 – Accepted: 16 March 2023 – Published: 14 April 2023

Abstract. Strontium isotopes ($^{87}Sr/^{86}Sr$) are useful to trace processes in the Earth sciences as well as in forensic, archaeological, palaeontological, and ecological sciences. As very few large-scale Sr isoscapes exist in Australia, we have identified an opportunity to determine $^{87}Sr/^{86}Sr$ ratios on archived fluvial sediment samples from the low-density National Geochemical Survey of Australia. The present study targeted the northern parts of Western Australia, the Northern Territory, and Queensland, north of 21.5° S. The samples were taken mostly from a depth of ∼ 60–80 cm in floodplain deposits at or near the outlet of large catchments (drainage basins). A coarse (< 2 mm) grain-size fraction was air-dried, sieved, milled, and digested (hydrofluoric acid + nitric acid followed by aqua regia) to release *total* Sr. The Sr was then separated by chromatography, and the $^{87}Sr/^{86}Sr$ ratio was determined by multicollector inductively coupled plasma mass spectrometry. The results demonstrate a wide range of Sr isotopic values (0.7048 to 1.0330) over the survey area, reflecting a large diversity of source rock lithologies, geological processes, and bedrock ages. The spatial distribution of $^{87}Sr/^{86}Sr$ shows coherent (multi-point anomalies and smooth gradients), large-scale (> 100 km) patterns that appear to be broadly consistent with surface geology, regolith/soil type, and/or nearby outcropping bedrock. For instance, the extensive black clay soils of the Barkly Tableland define a > 500 km long northwest–southeast-trending unradiogenic anomaly ($^{87}Sr/^{86}Sr < 0.7182$). Where sedimentary carbonate or mafic/ultramafic igneous rocks dominate, low to moderate $^{87}Sr/^{86}Sr$ values are generally recorded (medians of 0.7387 and 0.7422, respectively). Conversely, In proximity to the outcropping Proterozoic metamorphic basement of the Tennant, McArthur, Murphy, and Mount Isa geological regions, radiogenic $^{87}Sr/^{86}Sr$ values (> 0.7655) are observed. A potential correlation between mineralization and elevated $^{87}Sr/^{86}Sr$ values in these regions needs to be investigated in greater detail. Our results to date indicate that incorporating soil/regolith Sr isotopes in regional, exploratory geoscience investigations can help identify basement rock types under (shallow) cover, constrain surface processes (e.g. weathering and dispersion), and, potentially, recognize components of mineral systems. Furthermore, the resulting Sr isoscape and future models derived therefrom can also be utilized in forensic, archaeological, palaeontological, and ecological studies that aim to investigate, for example, past and modern animal (including humans) dietary habits and migrations. The new spatial Sr isotope dataset for the northern Australia region is publicly available (de Caritat et al., 2022a; https://doi.org/10.26186/147473).

Published by Copernicus Publications.

1 Introduction

Strontium isotope ratios ($^{87}Sr/^{86}Sr$) can be measured in many geological materials, as the trace element strontium (Sr) is relatively abundant and readily substitutes for calcium (Ca) in minerals and organic tissues. The $^{87}Sr/^{86}Sr$ of a mineral or rock is a function of (1) its initial and unchanging ^{86}Sr content, (2) its initial rubidium (Rb) content (thus Rb/Sr ratio), and (3) time (e.g. McNutt, 2000). Rubidium substitutes readily for potassium (K) in minerals and is, thus, also relatively common. As one of the two naturally occurring Rb isotopes, ^{87}Rb, which accounts for 27.8 % of Rb, decays over time (by emitting a negative beta particle) to stable ^{87}Sr ($t_{1/2} = 49.6 \times 10^9$ years), and the $^{87}Sr/^{86}Sr$ ratio of that material slowly increases with time (e.g. Rotenberg et al., 2012; Nebel and Stammeier, 2018). During geological processes, such as mineral dissolution or precipitation, or biological processes, such as bone and tooth growth, the $^{87}Sr/^{86}Sr$ remains constant, as there is no fractionation (e.g. Gosz et al., 1983; Nebel and Stammeier, 2018). These characteristics make the Sr isotopic system very useful in the geosciences, where it has been used for decades, for instance, in the study of the following:

- sediment diagenesis and low-grade metamorphism (e.g. Swart et al., 1987; Schultz et al., 1989; Mountjoy et al., 1992; Schaltegger et al., 1994);
- sediment, dust, and soil provenance (e.g. Douglas et al., 1995; Revel-Rolland et al., 2006; Bathgate et al., 2011; Bataille and Bowen, 2012; De Deckker et al., 2014; Jomori et al., 2017; De Deckker, 2020; de Caritat et al., 2022b);
- stratigraphy and reservoir/basin analysis (e.g. Rundberg and Smalley, 1989; Smalley et al., 1989, 1992; McArthur et al., 2012);
- fluid flow (e.g. McNutt et al., 1987; Stueber et al., 1987; Sullivan et al., 1990; Bagheri et al., 2014);
- weathering and pedogenesis (e.g. Åberg et al., 1989; Faure and Felder, 1981; Wickman and Jacks, 1992; Blum et al., 1994; Bullen et al., 1994, 1997; Quade et al., 1995; Probst et al., 2000; Harrington and Herczeg, 2003; Oliver et al., 2003; Green et al., 2004);
- terrestrial ecosystems and catchment processes (e.g. Graustein, 1989; Jacks et al., 1989; Lyons et al., 1995; Négrel and Grosbois, 1999; Négrel and Pauwels, 2004; Gosselin et al., 2004; Chadwick et al., 2009; Hagedorn et al., 2011);
- hydrology and hydrogeology (e.g. Collerson et al., 1988; Andersson et al., 1992, 1994; Douglas et al., 1995; Yang et al., 1996; Grobe et al., 2000; Dogramaci and Herczeg, 2002; Ojiambo et al., 2003; Palmer et al., 2004; Cartwright et al., 2007; Christensen et al., 2018; Shin et al., 2021);
- environment and environmental change (e.g. Andersson et al., 1990; Åberg, 1995; Åberg et al., 1995; Oishi, 2021);
- (palaeo)climatology and palaeogeographic reconstructions (e.g. Blum and Erel, 1995; Wei et al., 2018; Flecker et al., 2002);
- determining the $^{87}Sr/^{86}Sr$ of seawater through geological time (e.g. Veizer, 1989; Gruszczynski et al., 1992; Denison et al., 1994a, b; Shields, 2007); and
- ore genesis and mineral exploration (e.g. Le Bas et al., 1997; de Caritat et al., 2005; Daneshvar et al., 2020; Wei et al., 2020; Zhao et al., 2021).

Outside of the geosciences, food tracing and provenancing have also been underpinned by the use of Sr isotopes, although, in this case, generally relying on the *bioavailable* Sr rather than the total Sr (e.g. Voerkelius et al., 2010; Di Paola-Naranjo et al., 2011; Vinciguerra et al., 2015; Hoogewerff et al., 2019; Moffat et al., 2020). Anthropological studies have relied on $^{87}Sr/^{86}Sr$ isotope ratios to locate archaeological artefacts or reconstruct ancient human behaviours (e.g. Frei and Frei, 2013; Willmes et al., 2014, 2018; Adams et al., 2019; Pacheco-Forés et al., 2020; Washburn et al., 2021). Animal migration studies have also relied on Sr isotope data (e.g. Price et al., 2017). More recently, large-scale compilations and machine-learning-based predictions of the $^{87}Sr/^{86}Sr$ variations up to the continental and even global scale have been proposed (e.g. Bataille et al., 2014, 2018, 2020).

Strontium isotope landscape maps ("isoscapes") provide the fundamental context required for the interpretation of more detailed scientific research about processes or provenance. Despite the plethora of research using Sr isotopes to address various scientific questions, very few Sr isoscapes exist in the Southern Hemisphere, particularly for soils or covering large swathes of the Earth's surface (see Bataille et al., 2020). Two exceptions to this are (1) the work by Adams et al. (2019), which reported $^{87}Sr/^{86}Sr$ in plant, soil, and biota over $\sim 300\,000\,km^2$ on the Cape York Peninsula in Australia, and (2) the $\sim 500\,000\,km^2$ Sr isoscape of inland southeastern Australia recently published by our team (de Caritat et al., 2022b). The present study affords an opportunity to further redress this deficiency and will reduce the Northern Hemisphere bias in future global $^{87}Sr/^{86}Sr$ models. It also pertains to a land surface that has not been rejuvenated by recent glaciation, consisting of over 85 % regolith or weathered material (Wilford, 2012), and, as a result, is abundant in minerals such as kaolinite, illite–smectite, goethite, and hematite. The choice of total rather than bioavailable Sr as the focus of this work was driven by an emphasis on geological sources and processes.

2 Setting

The study area in northern Australia stretches across Western Australia, the Northern Territory, and Queensland (hereafter abbreviated to WA, NT, and Qld, respectively), north of 21.5° S (Fig. 1). It is surrounded by the Indian Ocean to the west, the Timor and Arafura seas and the Gulf of Carpentaria to the north, and the Coral Sea (Pacific Ocean) to the east. The main climate zones in the area are described as "Hot humid summer" in the north and along the coast and "Warm humid summer" further south and inland (Bureau of Meteorology, 2022a). The vegetation zones are dominated by "Tropical savanna" and "Hot grassland with winter drought" (Bureau of Meteorology, 2022b). The 10-year (1996–2005) average minimum and maximum temperatures mostly range from 15 to 24 °C and from 27 to 36 °C, respectively (Bureau of Meteorology, 2022c). Average annual rainfall over the 4-year period to November 2009 (when the bulk of the sampling was completed) mostly ranges from 400 to 1500 mm yr^{-1} and is strongly seasonal (summer rain) (Bureau of Meteorology, 2022d). Physiographically, the study area includes, from west to east, the Kimberley, North Australian Plateaus, Barkly–Tanami Plains, Carpentaria Fall, Carpentaria Lowlands, Peninsular Uplands, and Burdekin Uplands provinces (Pain et al., 2011). Topographic altitude ranges from sea level to 1622 m a.s.l. (above sea level) at Mount Bartle Frere (Qld's highest point, located just south of Cairns), and the mean altitude is ∼ 260 m a.s.l. (Geoscience Australia, 2008).

The soil types most commonly encountered in the study area are, according to the Australian Soil Classification scheme (Isbell and National Committee on Soil and Terrain, 2021; Australian Soil Resource Information System, 2022a), Vertosol, Kandosol, or Tenosol (∼ 24 % of the sample sites each), followed by Rudosol, Hydrosol, or Sodosol (7 %–9 %) and the rarer Calcarosol, Chromosol, Dermosol, or Podosol (< 2 %). The major river basins that divide the area belong, from west to east, to the Pilbara, Sandy Desert–Mackay, Fitzroy, North Kimberley, Ord, Victoria, Tennant, Daly, Darwin, Melville, Alligator, Roper, Arnhem, McArthur, Channel Country, Burketown, Leichhardt, Flinders, Gilbert, Weipa, Mitchell, Princess Charlotte Bay, Burdekin, Barron, Cooper Creek, and Whitsunday water regions (Geoscience Australia, 1997). Land use over the area is overwhelmingly "Grazing natural vegetation", followed by "Other protected areas (inc. indigenous uses)" and "Nature conservation" (Australian Soil Resource Information System, 2022b).

The main geological region groups (Blake and Kilgour, 1998) over the study area are, from west to east, the Pilbara, Canning, Kimberley, Bonaparte, Ord, Victoria, Pine Creek, Victoria, Wiso, Arunta–Tanami, Tennant, Money, McArthur, Arafura, Georgina, Isa, Carpentaria, Eromanga, Georgetown–Coen, Quinkan, and Paleozoic-Qld groups (see Fig S1 in the Supplement). The higher-level geological region domains (Blake and Kilgour, 1998) over the study area are, from west to east, the Pilbara, Paleozoic, North Australian Craton, Proterozoic, and Meso-Cenozoic domains (see Fig S2 in the Supplement). Thus, the study area displays a complex and protracted geological history spanning over 3.6 Gyr (Ollier, 1988; Braun et al., 1998; Betts et al., 2002; Blewett, 2012; Withnall et al., 2013; Ahmad and Scrimgeour, 2013), with two cratonic nuclei in the west and centre (the Archean Pilbara Craton and Palaeoproterozoic–Mesoproterozoic North Australian Craton) flanked by younger Proterozoic and Palaeozoic orogenic belts and basins, including the Phanerozoic Tasmanides to the east. Mesozoic and Cenozoic sedimentary sequences of the Eromanga and Carpentaria basins conceal much of the basement terrain over the eastern third of the study area. The whole region has experienced extensive weathering, resulting in a ubiquitous and locally thick regolith mantle.

Figure 2a shows that the decidedly dominant bedrock unit intersected by the sample sites is "Sedimentary and low-grade metamorphics" (89 % of sites), followed by the much less frequent "Felsic igneous intrusive" (4 %) and "Mafic to ultramafic igneous volcanic" (3 %) lithologies. Representing 2 % or less each are the "Medium-grade metamorphics", "Felsic to mafic igneous volcanic", "High-grade metamorphics", "Mafic igneous intrusive", and "Felsic to intermediate igneous volcanic" lithologies. Further investigation of the dominant bedrock unit "Sedimentary and low-grade metamorphics" reveals that it is comprised of "Regolith" (79 %), "Sedimentary siliciclastic" (4 %), "Feldspar- or lithic-rich arenite to rudite" (2 %), "Sedimentary carbonate" (2 %), and < 1 % each of "Argillaceous detrital sediment", "Metasedimentary siliciclastic", and "Quartz-rich arenite to rudite". Further, the "Regolith" class is reported to mainly consist of "Alluvium" (51 %), "Sand plain" (9 %), "Estuarine and delta deposit" (4 %), "Colluvium" (4 %), "Calcrete" (3 %), "Undifferentiated sediment" (3 %), "Lake deposit" (2 %), and < 2 % each of "Black soil plain", "Dune", and "Ferruginous duricrust".

The bedrock ages (periods) intersected at the sample sites are overwhelmingly Tertiary–Quaternary (58 %), followed by much less frequent Mesoproterozoic (8 %), Cenozoic (6 %), Cambrian (5 %), Palaeoproterozoic (5 %), Palaeoproterozoic–Mesoproterozoic (3 %), Carboniferous–Permian (3 %), Permian (3 %), Devonian–Carboniferous (2 %), Archaean (2 %), and Cambrian–Ordovician (2 %) ages. Representing < 2 % are the Devonian, Jurassic–Cretaceous, Ordovician, Silurian–Devonian, Jurassic, Neoproterozoic–Cambrian, and Triassic periods.

Numerous mineral occurrences are found in northern Australia, and Fig. 2b shows the most important ones classified as "Mineral Deposits" (i.e. those with an inferred resource), "Operating Mines" (currently producing), or "Developing Projects" (approved but not yet producing). As mineralization is the end point of geologically "unusual" processes taking place regionally in "mineral systems" (Wyborn et al., 1994), it is useful to investigate if mineral system processes leave a recognizable $^{87}Sr/^{86}Sr$ fingerprint in the country rock

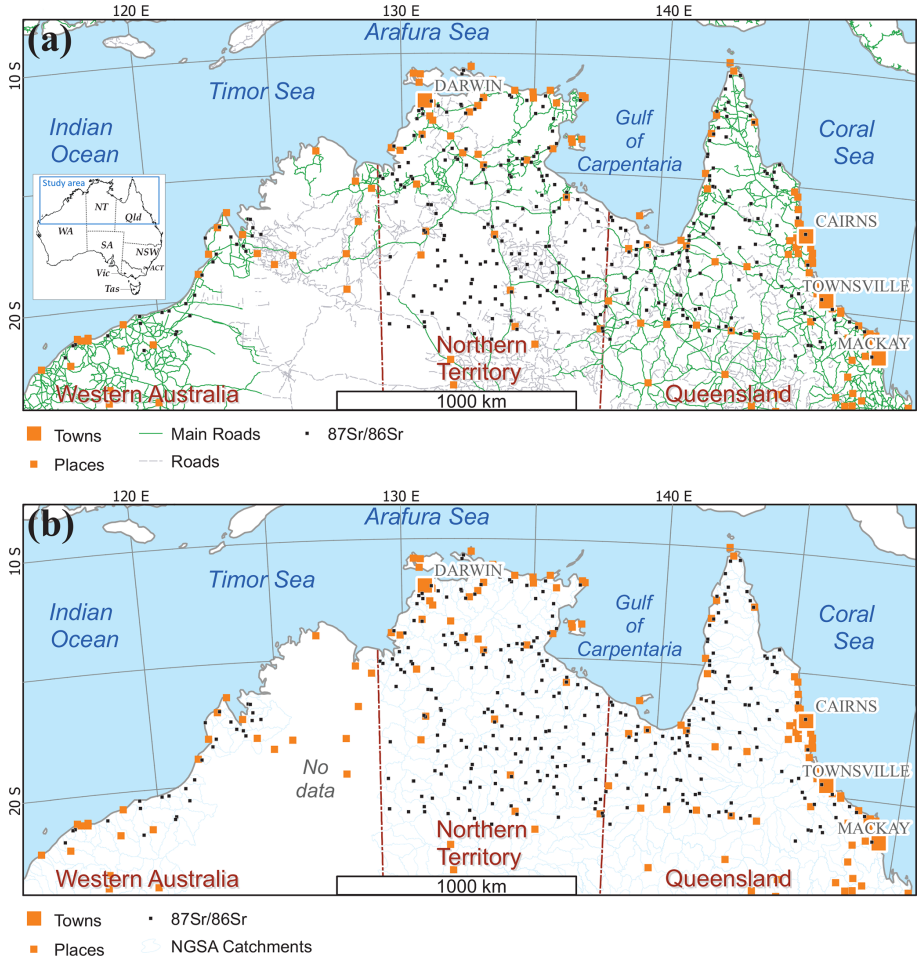

Figure 1. The northern Australia Sr isotope study area (see the inset for location: WA – Western Australia, NT – Northern Territory, Qld – Queensland, NSW – New South Wales, ACT – Australian Capital Territory, Vic – Victoria, Tas – Tasmania, and SA – South Australia) and the National Geochemical Survey of Australia (NGSA) and Northern Australia Geochemical Survey (NAGS) $^{87}Sr/^{86}Sr$ sample locations (small black squares) shown with towns (large orange squares) and places (medium orange squares), main roads (solid green lines in panel **a**), secondary roads (dashed grey lines in panel **a**), and the NGSA catchment boundaries (medium blue lines in panel **b**). Map projection: Albers equal area.

and sediment derived therefrom. The study area is particularly rich in "Base Metals" deposits (both Pb–Zn- and Cu-dominated deposits, e.g. the Mount Isa, McArthur River, and George Fisher deposits) and is host to the "North Australian Zinc Belt", the world's largest Zn–Pb province (Huston et al., 2022). In addition, notable occurrences of "Battery or Alloy Metals" (Ni, Co, Mn, V, Mo, and Mg, e.g. the Spinifex Ridge, Ripon Hills, Julia Creek, and Richmond deposits) and "Precious Metals" (Au and Ag, e.g. the Mount Isa and George Fisher deposits) are also found here. Further, "Other Metals" (Sn, Sb, W, Ta, and Nb, e.g. the Mount Carbine deposit), "Rare Earth Elements" (e.g. Thunderbird and Nolans Bore deposits), "Platinum Group Elements" (Pt, Pd, and Rh, e.g. the Munni Munni deposit), and "Heavy Mineral Sands" (e.g. Thunderbird deposit) occurrences are also catalogued. Thus, the area is significant for underpinning Australia's critical mineral resources supply now and into the future (e.g. Department of Industry, Science, Energy and Resources, 2022), without which a global transition to a lower-carbon economy will be challenging.

3 Material and methods

3.1 Material

This study makes use of archive "catchment outlet sediment" samples collected during the National Geochemical Survey of Australia (NGSA), which covered ~ 80 % of Australia (de Caritat and Cooper, 2011a, 2016; de Caritat, 2022). The sampling philosophy of the NGSA was to collect naturally mixed and fine-grained fluvial/alluvial sediments from large catchments, thereby obtaining a representative average of the main soil and rock types contributing sediment through weath-

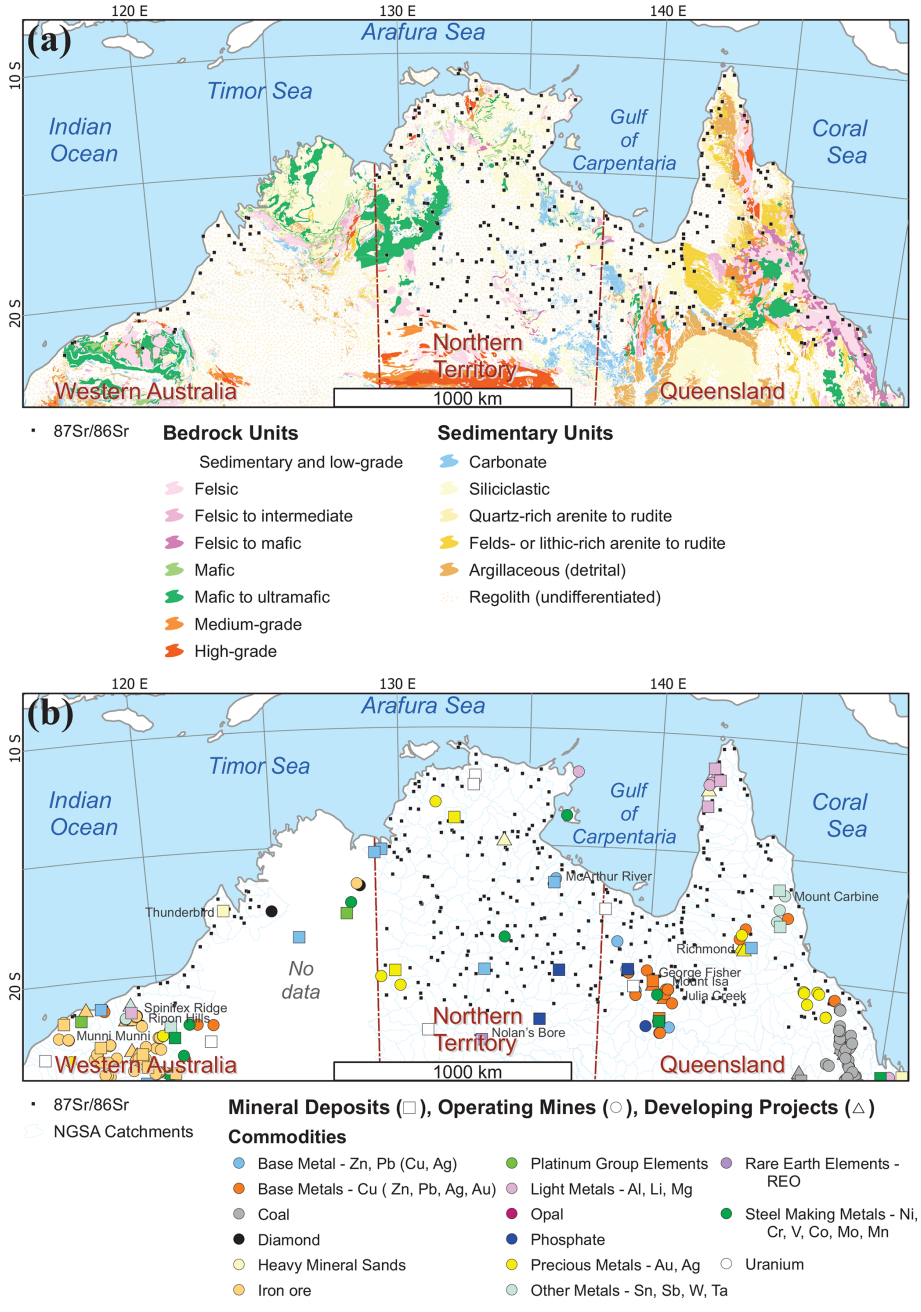

Figure 2. The northern Australia Sr isotope study area and National Geochemical Survey of Australia (NGSA) and Northern Australia Geochemical Survey (NAGS) $^{87}Sr/^{86}Sr$ sample locations (small black squares) shown with **(a)** surface geology from Raymond et al. (2012) and **(b)** NGSA catchment boundaries (medium blue) and mineral occurrences (Geoscience Australia, 2022a). Map projection: Albers equal area.

ering. This allowed an ultralow sampling density (approximately one sample per 5200 km^2) that was still representative of large-scale natural variations (de Caritat and Cooper, 2011b). Catchment outlet sediments are similar to floodplain sediments in the sense that they are deposited during receding floodwaters outside the riverbanks; however there is an added complexity in that, in Australia, many areas can also experience the addition (or loss) of aeolian material. The sampled floodplain geomorphological entities are typically vegetated and biologically active (e.g. plants, worms, and ants), thereby making the collected materials true soils, albeit soils developed on transported alluvium parent material.

The sampling medium and density were both strategically chosen in the NGSA project to prioritize coverage over resolution. This was justified by the fact that the NGSA was Australia's first and, to date, only fully integrated, internally

consistent geochemical survey with a truly national scope. In terms of the present study area, it is clear that these choices have implications with respect to the granularity of the patterns revealed by the Sr isoscape; as the collection of Sr isotope data in Australia using NGSA samples grows in the future (e.g. de Caritat et al., 2022b, and this contribution), it is hoped that the value of coverage will prevail over a relative low resolution of detailed features.

The NGSA collected samples at two depths: a "top outlet sediment" (TOS) from a shallow (0.1 m) soil pit approximately 0.8 m × 0.8 m in area and a "bottom outlet sediment" (BOS) from a minimum of three auger holes that were generally drilled within ∼ 10 m of the TOS pit. The auger holes were drilled as deep as possible (to refusal or to a maximum depth of 1 m), and the BOS sample was collected from an average depth of 0.6–0.8 m from all drilled holes. A field manual was compiled to record all sample collection method details, including site selection (Lech et al., 2007). Sampling for the NGSA took place between July 2007 and November 2009, and the field data were recorded in Cooper et al. (2010). In the laboratory, the samples were air-dried at 40 °C for a minimum of 48 h (or to constant mass) before being further prepared (see de Caritat et al., 2009); for the comprehensive geochemical analysis programme of the NGSA, the reader is referred to de Caritat et al. (2010). An aliquot of a minimum of ∼ 1 g of sample was milled to a fine powder using a carbon steel ring mill or, for a few samples only, an agate micromill. The main sample type selected for the present Sr isotope study was NGSA BOS < 2 mm in order to be as representative as possible of the geogenic background unaffected by modern land use practices and inputs (e.g. fertilizers). A few NGSA TOS < 2 mm samples, prepared in an identical fashion, were also analysed.

Several additional samples from the Northern Australia Geochemical Survey (NAGS; Bastrakov and Main, 2020) were included in this project, as they provide a higher-density coverage over part of the study area. The NAGS project used the same sampling philosophy and sample collection, preparation, and analysis methods as the NGSA, with a higher sampling density of one sample per ∼ 500 km^2. The NAGS project collected only TOS (0–0.1 m depth) samples, and the NAGS TOS < 2 mm aliquots were prepared and analysed as per the NGSA samples. Sampling for the NAGS took place in May and June 2017.

Overall, 326 NGSA BOS < 2 mm, 18 NGSA TOS < 2 mm (including 15 with BOS also analysed), and 28 NAGS TOS samples, resulting in a total of 372 analyses from 357 samples, were analysed for Sr isotopes as detailed in Sect. 3.2 below. Given that there are ∼ 10 % field duplicates in the NGSA and the smaller NAGS catchments are nested within NGSA catchments, all of those samples originate from within 307 NGSA catchments, which together cover 1.536 × 10^6 km^2 of northern Australia (see Fig. 1).

3.2 Methods

Samples were prepared and analysed for Sr isotopes ($^{87}Sr/^{86}Sr$) at the Wollongong Isotope Geochronology Laboratory (WIGL). Approximately 50 mg of sample was weighed and digested in a 2 : 1 mixture of hydrofluoric and nitric acids. All reagents used were SEASTAR™ BASELINE® grade, with Sr concentrations typically < 10 ng kg^{-1}. Following digestion, samples were redissolved in aqua regia (twice if needed) in order to eliminate any fluorides, followed by nitric acid twice. Finally, samples were redissolved in 2 M nitric acid prior to ion exchange chromatography. Strontium was isolated from the sample matrix using an automated, low-pressure chromatographic system (Elemental Scientific prepFAST MC™) and a 1 mL Sr–Ca column (Eichrom™) (Romaniello et al., 2015). The Sr elutions were redissolved in 0.3 M nitric acid. Strontium isotope analysis was performed on a Neptune Plus™ (ThermoFisher Scientific) multicollector inductively coupled plasma mass spectrometer (MC-ICP-MS) at WIGL. The sample introduction system consists of Apex-ST PFA MicroFlow nebulizer (Elemental Scientific, Inc.) with an uptake rate of ∼ 0.1 mL min^{-1}, a quartz SSI dual cyclonic spray chamber, jet sample, and X-skimmer cones. Measurements were performed in low-resolution mode. The instrument was tuned at the start of each session with a 20 µg kg^{-1} Sr solution, and sensitivity for ^{88}Sr was typically around 4 V. Masses 88, 87, 86, 85, 84, and 83 were collected on Faraday cups. Instrumental mass bias was internally corrected using measured $^{87}Sr/^{86}Sr$. Masses 85 and 83 were used to correct for the isobaric interference of ^{87}Rb and ^{86}Kr, respectively. Maps were prepared using the open software QGIS® (version 3.16.14 Hannover) and applying an Albers equal area projection. Symbology for displaying $^{87}Sr/^{86}Sr$ data here either classified point data in eight equal quantile classes (12.5 % of the data each, using a gradient from green denoting low to red denoting high) at the sampling site or attributed the same value and colour to the whole catchment from which the outlet sediment comes, reflecting the sampling medium, catchment outlet sediment, being a representative sample of the average materials in the catchment (see Sect. 3.1).

3.3 Quality assessment

National Institute of Standards and Technology (NIST) strontium carbonate isotope Standard Reference Material SRM987 was used as a secondary standard and measured after every five samples to assess accuracy during analysis. The accuracy of the whole procedure was assessed by processing United States Geological Survey (USGS) reference material basalt from the Columbia River standard BCR-2 (Plumlee, 1998). The mean ±2 standard errors $^{87}Sr/^{86}Sr$ value for BCR-2 in this study is 0.704961 ± 35 ($n = 13$), which is within the error of the value in Jweda et al. (2016) (0.704500 ± 11). Total procedure blanks ranged between

0.025 and 0.245 ng Sr ($n = 12$). A total of 20 field duplicate sample pairs (collected at a median distance of ∼ 80 m from one another on the same landscape unit; see Lech et al., 2007) were analysed for $^{87}Sr/^{86}Sr$ in the BOS < 2 mm sample, and they returned a median relative standard deviation of 0.17 %. The relative standard deviation from field duplicates includes natural variability (mineralogical/chemical heterogeneity of the alluvial deposit) as well as sample collection, preparation, and analysis uncertainties.

Overall, we feel that the quality of the $^{87}Sr/^{86}Sr$ data presented herein is adequate for the purpose of regional mapping and that reporting $^{87}Sr/^{86}Sr$ data to the third decimal place with an indicative fourth decimal place is appropriate for this work. This relatively low precision obtained for field duplicates is attributed to the heterogeneity of the alluvial deposits, as precision relating to sample preparation and analysis for Sr isotopes is at the fifth decimal place (see the results for BCR-2 above).

3.4 Data analysis

Data management was performed using Microsoft Excel®, graphing and visualization was carried out using IMDEX ioGas®, and spatial analysis and mapping was undertaken with QGIS® (an open-source geographical information system). For the purposes of generating the Sr isoscape from combined BOS and TOS samples, calculated "BOS-equivalent" values of TOS were derived from regression analysis (see Sect. 5.2). Catchment-based Sr isoscapes were constructed by assigning the $^{87}Sr/^{86}Sr$ value of a catchment's outlet sediment sample to each corresponding NGSA catchment or, if more than one sample was analysed per catchment (e.g. field duplicates or higher-resolution NAGS samples), by assigning the mean of those multiple samples. All maps are shown in Albers equal area projection.

4 Results

The soil $^{87}Sr/^{86}Sr$ values reported herein range from 0.7048 to 1.0330 (range = 0.3282). The median is 0.7405 and the mean is 0.7532 (standard deviation = 0.0480; kurtosis = 8.1602; skewness = 2.4640). Figure 3 illustrates the univariate structure of the new data. Spatially, the $^{87}Sr/^{86}Sr$ values define large-scale, coherent patterns with multi-point low and high regions (Fig. 4). The main high-value (radiogenic) regions are found in the central and northern parts of the NT, most of Cape York, and along some of the coast (including the WA part of the study). Prominent low-$^{87}Sr/^{86}Sr$-value (unradiogenic) regions include a large, central, northwest–southeast-trending elongated area in the NT, a smaller and similarly trending area in central Qld, and the northernmost and easternmost parts of the Qld study area.

5 Discussion

5.1 Comparison with other datasets

A comparison of the present results with selected soil $^{87}Sr/^{86}Sr$ datasets from around the world is offered in Table 1. All discoverable data from Australia and the Southern Hemisphere comprising more than a handful of sites were included, whereas only selected Northern Hemisphere datasets focusing on recent and large-scale datasets were included. Table 1 combines both bioavailable/exchangeable and bulk/-total $^{87}Sr/^{86}Sr$ data, representing variable soil grain-size fractions (where reported), parent materials, and land uses. Despite this variability, one can make several observations. Firstly, the northern Australia Sr isotope dataset has the highest maximum (1.0330) and largest range (0.3282) of $^{87}Sr/^{86}Sr$ values amongst those compiled. Secondly, there is no observed standard protocol for collecting or preparing soils for either bioavailable or total $^{87}Sr/^{86}Sr$ determination. Thirdly, total $^{87}Sr/^{86}Sr$ datasets tend to have a wider range and greater variance than bioavailable ones, at least partly accounting for the higher values encountered here. These issues complicate data compilation and integration across projects/-countries but do not preclude them. Indeed, through contemporaneous data analytics, including artificial intelligence and machine learning, it is likely that the relationships between bioavailable and total Sr isotope values and a host of other environmental variables (including from climatic, topographic, biotic, and geoscientific categories) can be teased out and that high-spatial-resolution models/predictions of bioavailable or total Sr isotope distribution can be derived (e.g. Bataille et al., 2020). This is indeed a future research direction that we propose/support for isoscape science in general as well as in an Australian Sr isoscape in particular.

5.2 Top–bottom relationship

Based on the 15 sites where both TOS and BOS samples were analysed, a strong correlation (Fig. 5) between the aforementioned two depths is found:

$$(^{87}Sr/^{86}Sr)_{BOS} = 0.9913 \times (^{87}Sr/^{86}Sr)_{TOS} + 0.0069 \ (r^2 = 0.97;\ p < 0.001;\ n = 15). \quad (1)$$

Equation (1) was used to infer BOS $^{87}Sr/^{86}Sr$ from those sites where only TOS samples could be obtained (i.e. 3 NGSA and 28 NAGS sites), effectively deriving a BOS-equivalent $^{87}Sr/^{86}Sr$ value for the purposes of performing internally consistent statistical and spatial analysis.

As a result of the robust correlation between TOS and BOS, the BOS (or subsurface) Sr isoscapes of Fig. 4 can be recalculated to TOS (or surface) Sr isoscapes by replacing the legend values for the eight quantile class boundaries with the values 0.7050–0.7156–0.7215–0.7293–0.7401–0.7522–0.7674–0.7910–1.0276. A TOS map and values would be useful when studying surface processes, such as plant and

https://doi.org/10.5194/essd-15-1655-2023

Table 1. Comparison of $^{87}Sr/^{86}Sr$ data from this study with selected datasets from around the world, with an emphasis on Australia and the Southern Hemisphere (count, minimum, median, mean, standard deviation, maximum, and range). The regions are abbreviated as follows: Aus – Australia, Qld – Queensland, SA – South Australia, SE – southeastern, Vic – Victoria, and WA – Western Australia. The digestions are abbreviated as follows: AcAc – acetic acid (CH_3COOH), AmAc – ammonium acetate (CH_3COONH_4), AmNt – ammonium nitrate (NH_4NO_3), and AR – aqua regia.

Region	Sample Type	Digestion	*n*	Min	Med	Mean	SD	Max	Range	Source
Southern Hemisphere: Aus										
Northern Aus	Soil (on alluvium), < 2 mm	Milled, HF + HNO_3 + AR	357	0.7048	0.7390	0.7527	0.0484	1.0330	0.3282	This study
SE Aus	Soil (on alluvium), < 2 mm	Milled, HF + HNO_3 + AR	112	0.7089	0.7199	0.7220	0.0736	0.7511	0.0422	de Caritat et al. (2022b)
Mostly SA, Vic (19 sites)	Soil (calcrete)	AcAc	26	0.7061	0.7102	0.7115	0.0051	0.7329	0.0267	Quade et al. (1995)
SE Aus; Murray–Darling Basin	Alluvium, < 2 µm	HF + HNO_3	26	0.7080	0.7163	0.7267	0.0188	0.7751	0.0672	Gingele and De Deckker (2005)
Southern Aus (eight sites)	Soil (calcrete)	AcAc	46	0.7094	0.7151	0.7168	0.0058	0.7374	0.0280	Dart et al. (2007)
	Soil (calcrete)	HNO_3 + HF + HCl	38	0.7125	0.7382	0.7538	0.0588	0.9985	0.2860	Dart et al. (2007)
Canning Coast, WA	Dust, < 2 µm	AcAc	14	0.7141	0.7361	0.7385	0.0163	0.7727	0.0586	De Deckker (2019)
Cape York Peninsula, Qld	Soil, < 2 mm	AcAc	93	0.7075	0.7227	0.7252	0.0154	0.7911	0.0835	Adams et al. (2019)
Southern Hemisphere: Other										
Brazil (three regions)	Soil (agricultural), < 2 mm	AmAc	3	0.7122	0.7132	0.7129	0.0006	0.7133	0.0011	de Almeida (2021)
Southern Chile	Soil (forest)	AmAc	22	0.7091	0.7098	0.7101	0.0007	0.7119	0.0029	Kennedy et al. (2002)
Southern Peru	Soil (agricultural)	Ashed, AmAc	114	0.7020	0.7076	0.7077	0.0017	0.7189	0.0169	Knudson et al. (2014)
South Africa (four regions)	Soil (agricultural), < 180 µm	HNO_3 + H_2O_2	67	0.7081	0.7130	0.7126	0.0020	0.7159	0.0078	Vorster et al. (2010)
Southern New Zealand	Soil, < 2 mm	AmNt	83	0.7040	0.7079	0.7078	0.0013	0.7112	0.0072	Adam Martin, personal communication (2021)
Northern Hemisphere										
Britain	Soil	H_2O	26	0.7074	0.7093	0.7092	0.0010	0.7115	0.0041	Evans et al. (2010)
France	Soil, < 2 mm	AmNt	524	0.7033	0.7113	0.7119	0.0042	0.7308	0.0275	Willmes et al. (2014)
Europe	Soil (grazing), < 2 mm	AmNt	565	0.7038	0.7090	0.7103	0.0052	0.7523	0.0485	Hoogewerff et al. (2019)
	Soil (agricultural), < 2 mm	AmNt	622	0.7038	0.7093	0.7112	0.0063	0.7596	0.0558	Hoogewerff et al. (2019)
Israel	Soil, < 2 mm	AmNt	60	0.7058	0.7086	0.7085	0.0008	0.7102	0.0044	Moffat et al. (2020)
Cambodia	Soil	Ashed, HF	60	0.7034	0.7115	0.7130	0.0060	0.7424	0.0389	Shewan et al. (2020)
	Soil	Ashed, AmNt	46	0.7037	0.7110	0.7117	0.0039	0.7204	0.0167	Shewan et al. (2020)
Japan	Soil, < 2 mm	H_2O_2	13	0.7067	0.7085	0.7088	0.0016	0.7129	0.0062	Oishi (2021)
Italy	Soil	Exchangeable and bulk	273	0.7053	0.7091	0.7099	0.0027	0.7238	0.0185	Lugli et al. (2022)

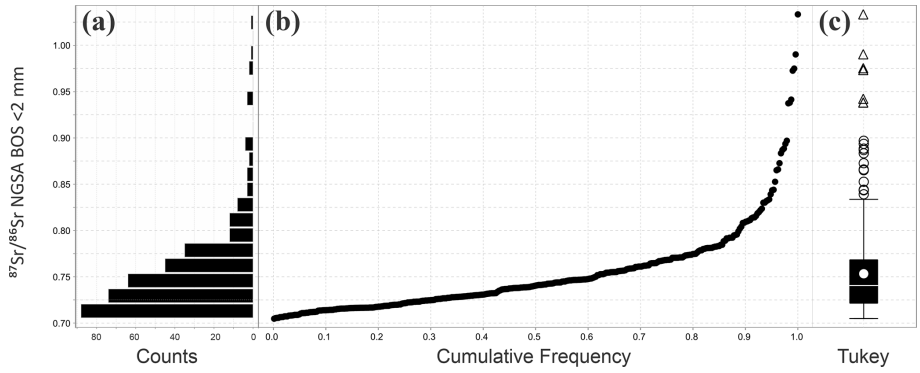

Figure 3. Univariate distribution of the $^{87}Sr/^{86}Sr$ data ($n = 357$) from the northern Australia Sr isotope study area: **(a)** histogram (20 bins, 0.016 wide); **(b)** cumulative frequency plot; and **(c)** Tukey box plot (the solid white dot shows the mean, circles denote outliers, and triangles represent extreme outliers) (Tukey, 1977). The sample medium is the < 2 mm fraction of NGSA bottom outlet sediment (BOS) or equivalent (see the text for further information).

animal uptake or the effect of land use on sediment composition and dynamics.

5.3 Relationship to bedrock

When grouped by age of their respective geological region, the new $^{87}Sr/^{86}Sr$ data show a general trend of increasing $^{87}Sr/^{86}Sr$ with increasing bedrock age, as illustrated by the box and scatter plots in Fig. 6. In Fig. 6, average numerical ages (mid-points between beginning and end ages) are attributed to each geological period group. The observed trend is consistent with that of the known controls on mineral (and rock) $^{87}Sr/^{86}Sr$ values, namely their age.

Another known control on Sr isotopic values is the Rb content, which, over time, contributes ^{87}Sr by radiogenic decay. Closer examination of the geology in the catchments with the 10 highest $^{87}Sr/^{86}Sr$ values indicates that they contain lithologies likely to be enriched in Rb relative to Sr (e.g. felsic, felsic-to-intermediate igneous rocks, and medium- to high-grade metamorphic rocks), as shown using detailed maps in the Supplement. Of the 5 top 10 $^{87}Sr/^{86}Sr$ values in the northern NT, 3 are from the Pine Creek geological region. The two northernmost of these (sample nos. 2007190099 and 2007191390) with $^{87}Sr/^{86}Sr$ values of 0.9413 and 0.9900, respectively, are in catchments downstream of 1780–1790 Ma I-type granite intrusions that have been reported to have $^{87}Sr/^{86}Sr$ values from 0.71 to 8.13, $^{87}Rb/^{86}Sr$ values from ~ 1 to 290, Rb concentrations of up to 956 mg kg^{-1}, and Sr concentrations of up to 459 mg kg^{-1} (Riley, 1980, their Table 1).

The elevated samples from the WA coast are also generally proximal to, or downstream of, felsic igneous lithologies (including the granitoid and gneiss underlying the Mallina Basin; Van Kranendonk et al., 2002) and are consistent with $^{87}Sr/^{86}Sr$ values reported for clay fraction sediments from the region by De Deckker (2019), as shown in the Supplement. The northernmost samples along the coast of WA overlap with the King Leopold Orogen, abutting the western flank of the Kimberley geological region. Few $^{87}Sr/^{86}Sr$ data are available for this region, but those that exist within the Hooper Complex (Griffin et al., 2000) indicate radiogenic $^{87}Sr/^{86}Sr$ values: 0.7708–0.9620 for the Whitewater Volcanics, 0.7336–0.8524 for the Kongorow Granite, and 0.7353–0.7602 for the Lennard Granite (Bennett and Gellatly, 1970, their Table 2). Thus, observed elevated $^{87}Sr/^{86}Sr$ values of 0.8080, 0.7709, and 0.7923 in three sediment samples (sample nos. 200719103, 2007190317, and 2007190966, respectively) near Derby, WA, are entirely compatible with these bedrock source rocks.

Page et al. (1980, their Table 5) published Rb and Sr data from Alligator Rivers uranium field rocks, including from the Nimbuwah Complex granitoid close to Cooper Creek, < 20 km north of the Nabarlek uranium deposit (their sample no. 7212.4063). For this sample, they reported $^{87}Rb/^{86}Sr$ values of 1.25–1.47, $^{87}Sr/^{86}Sr$ values of 0.7387–0.7442, Rb concentrations of 146–164 mg kg^{-1}, and Sr concentrations of 320–336 mg kg^{-1}. Our sample (sample no. 2007190710) from this same catchment has a $^{87}Sr/^{86}Sr$ value of 0.8019 and is located on a felsic granite polygon.

Black et al. (1983, their Tables 3 and 5) reported calculated initial rock $^{87}Sr/^{86}Sr$ ratios in the range from 0.76 to 0.92 from granites, including the Wangala and the Haverson granites, in the northern Arunta geological region (southern NT). These intrusions intersect three sampled NGSA catchments for which we obtained elevated $^{87}Sr/^{86}Sr$ values, namely 0.8140, 0.7763, and 0.8651 (sample nos. 2007190727, 2007190562, and 2007190123, respectively). These catchments are also just upstream of some of our top 10 $^{87}Sr/^{86}Sr$ values (between 0.8935 and 1.0330).

In the Georgetown geological region of northwestern Qld, broad consistency between whole-rock $^{87}Sr/^{86}Sr$ and catchment sediment $^{87}Sr/^{86}Sr$ is also observed. For instance, our sample no. 2007190858, from a catchment that drains mostly the Esmeralda Granite (average whole-rock initial $^{87}Sr/^{86}Sr$

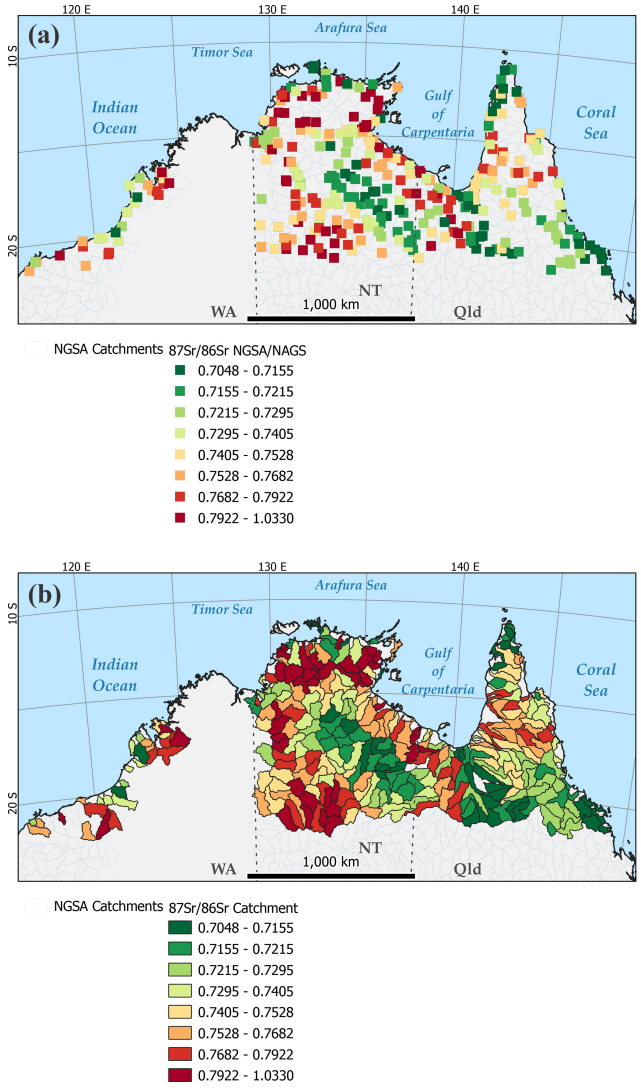

Figure 4. Strontium isoscape for the northern Australia study area with **(a)** data points classed by quantiles at the sampling sites and **(b)** as whole catchments coloured by same colour ramp. The sample medium is the < 2 mm fraction of NGSA bottom outlet sediment (BOS) or equivalent (see the text for further information). Map projection: Albers equal area.

of 0.7314 ± 0.0116; Black, 1973, their Table 2) on the western edge of the Georgetown Inlier, has a relatively elevated $^{87}Sr/^{86}Sr$ value of 0.7467. Conversely, the three catchments that mostly directly drain the less radiogenic Newcastle Range Volcanics in the centre of the Georgetown Inlier, which have a lower average whole-rock initial $^{87}Sr/^{86}Sr$ of 0.7152 ± 0.0011 (Black, 1973, Table 2), have correspondingly lower sediment $^{87}Sr/^{86}Sr$ values of 0.7318 (sample no. 2007190572), 0.7268 (sample no. 2007190348), and a field duplicate pair of 0.7258 (sample no. 2007190548) and 0.7282 (sample no. 2007190548).

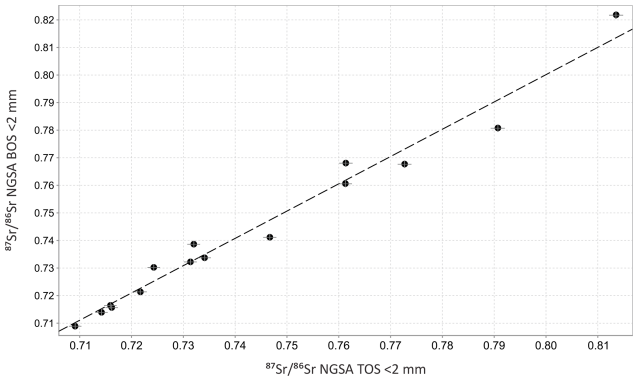

Figure 5. Scatterplot of the BOS (deep) versus TOS (surface) $^{87}Sr/^{86}Sr$ data ($n = 15$) from the northern Australia Sr isotope study area with total uncertainty derived from field duplicates (0.17 %; grey plus symbols) and linear square regression line (dashed line).

The floodplain sediment Sr isotopic values recorded in areas dominated by sedimentary carbonate and mafic/ultramafic igneous rocks are usually within an intermediate range between the more radiogenic and unradiogenic end-members discussed above. Indeed, samples sited within 0.1° (~ 10 km) of lithologies recorded as sedimentary carbonate and mafic/ultramafic igneous rocks have median values of 0.7387 ($n = 96$) and 0.7422 ($n = 42$), respectively.

5.4 Relationship to mineralization

Figure 7 illustrates the range of $^{87}Sr/^{86}Sr$ values of catchments that contain known mineralization of various types. A total of 44 NGSA catchments host 97 mineral occurrences as catalogued by Geoscience Australia (2022a). These resources include 19 "Base Metals – Zn, Pb (Cu, Ag)"; 17 "Battery/Alloy Metals – Ni, Co, Mn, V, Mo, Mg"; 13 "Precious Metals – Au, Ag"; 12 "Fertilizer Elements – P, K"; 6 "Rare Earth Elements"; 6 "Other Metals – Sn, Sb, W, Ta, Nb"; 5 "Iron Ore"; and 5 "Base Metals – Cu (Zn, Pb, Ag, Au)" occurrences. Whilst the vast majority of mineral occurrences are found in catchments with a sediment outlet $^{87}Sr/^{86}Sr$ signature $\ll 0.84$, six outlier occurrences are associated with higher catchment outlet sediment $^{87}Sr/^{86}Sr$ values: 0.8434 (the Coronation Hill Pt–Pd deposit in the catchment containing sample no. 2007191552); 0.9373 (Nolans Bore hard-rock rare earth element (REE) and Mount Peake vanadium deposits in the catchment containing sample no. 2007191112); 0.9748 (Batman Au deposit in the catchment containing sample no. 2007191329); and, highest of all, 0.9900 (the Browns Pb–Zn and the Browns Co deposits in the catchment containing sample no. 2007191387). Some mineral occurrence types are not found in catchments with $^{87}Sr/^{86}Sr$ signature less radiogenic than 0.75 in this study: the minima reported for the Platinum Group Elements, Rare Earth Elements/Heavy Mineral Sands, and Diamond com-

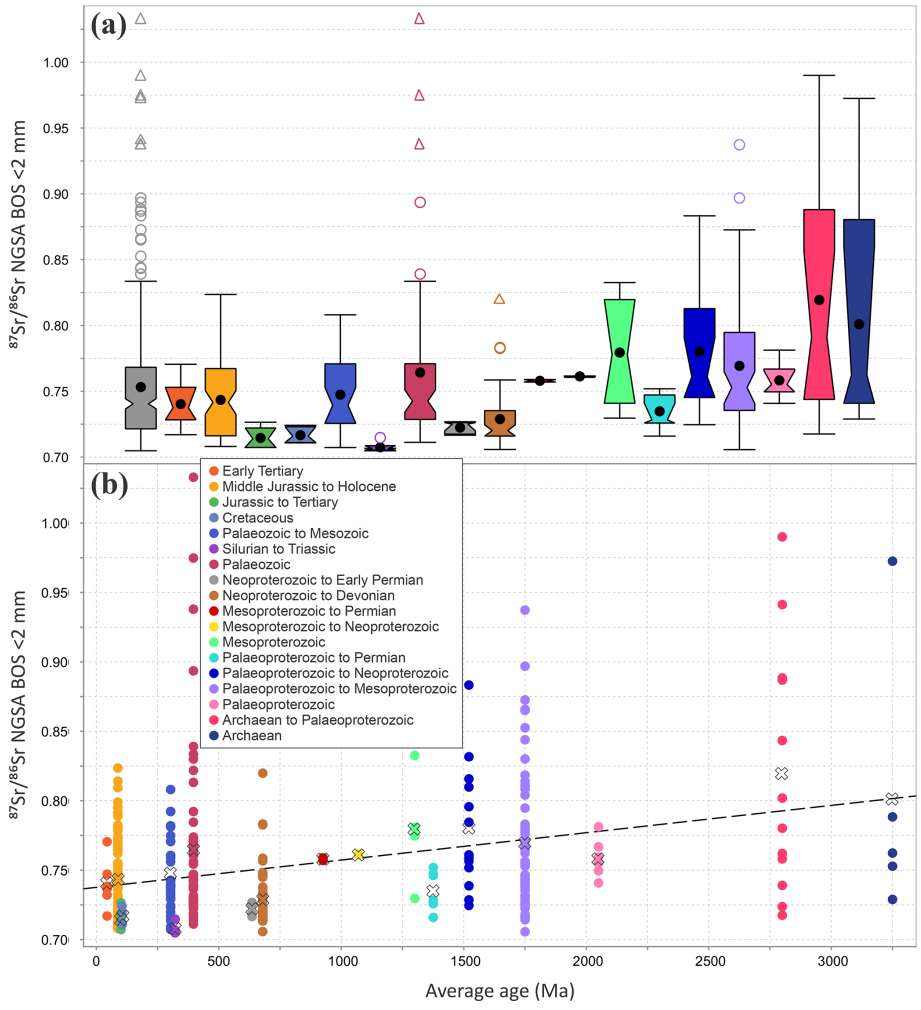

Figure 6. Distribution of the $^{87}Sr/^{86}Sr$ data from the northern Australia Sr isotope study area by geological region age: **(a)** notched Tukey box plots (Tukey, 1977) of, left to right, the whole dataset first (grey; $n = 357$) and then sorted by average age (early Tertiary, $n = 6$; Middle Jurassic to Holocene, $n = 80$; Jurassic to Tertiary, $n = 5$; Cretaceous, $n = 4$; Palaeozoic to Mesozoic, $n = 28$; Silurian to Triassic, $n = 6$; Palaeozoic, $n = 61$; Neoproterozoic to early Permian, $n = 7$; Neoproterozoic to Devonian, $n = 49$; Mesoproterozoic to Permian, $n = 2$; Mesoproterozoic to Neoproterozoic, $n = 2$; Mesoproterozoic, $n = 4$; Palaeoproterozoic to Permian, $n = 7$; Palaeoproterozoic to Neoproterozoic, $n = 13$; Palaeoproterozoic to Mesoproterozoic, $n = 59$; Palaeoproterozoic, $n = 7$; Archaean to Palaeoproterozoic, $n = 12$; and Archaean, $n = 5$); **(b)** a scatterplot against the average age of the geological region with the group averages (crosses) and linear square regression line (dashed line).

modity groups are 0.7529, 0.7606, 0.7606, and 0.7567, respectively. Whilst it is unlikely that mineral deposits themselves impart a significant control on the $^{87}Sr/^{86}Sr$ of sediment collected down-catchment given their usually limited size, the hosting country rock may, however, potentially be more widely affected by mineral system processes, and, upon further investigation, appears to record some Sr isotopic effect that may be useful for mineral vectoring. One of the most radiogenic $^{87}Sr/^{86}Sr$ signatures (0.9373) is found for the catchment hosting both the Mount Peake vanadium deposit (Simandl and Paradis, 2022) and the Nolans Bore hydrothermal REE deposit (Schoneveld et al., 2015). Hydrothermal or magmatic REE deposits are not usually characterized by highly radiogenic Sr signatures (e.g. 0.7029–0.7262 at Bayan Obo – Le Bas et al., 1997; 0.701–0.708 in global review of carbonatite deposits – Bolonin, 2019; and 0.7037–0.7062 at Caotan – Wei et al., 2020) and nor is Nolans Bore specifically (0.7054–0.7079; Huston et al., 2016). Thus, the elevated $^{87}Sr/^{86}Sr$ reported here from this catchment is attributed to the radiogenic bedrock occurring in the study area and perhaps in upstream catchments immediately to the south of it.

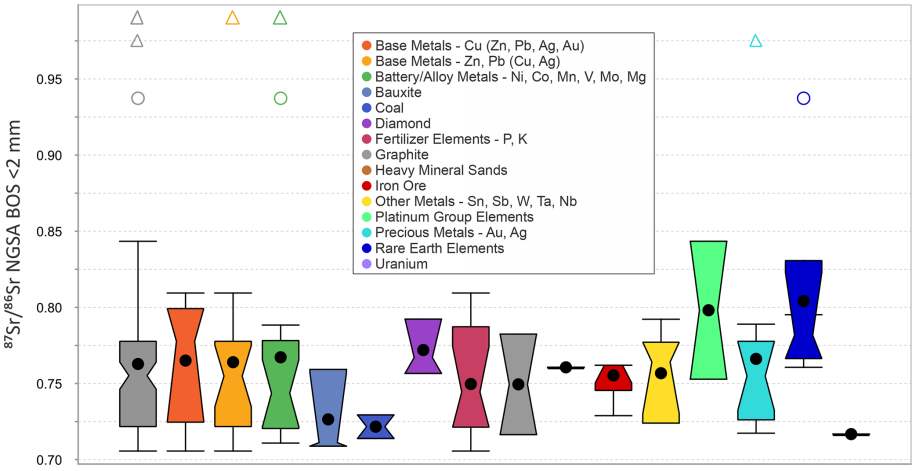

Figure 7. Distribution of the $^{87}Sr/^{86}Sr$ data from the northern Australia Sr isotope study area by mineral occurrence hosted in same catchment. The categories shown, from left to right, are as follows: all ($n = 97$); Base Metals – Cu (Zn, Pb, Ag, Au) ($n = 5$); Base Metals – Zn, Pb (Cu, Ag) ($n = 19$); Battery/Alloy Metals – Ni, Co, Mn, V, Mo, Mg ($n = 17$); Bauxite ($n = 3$); Coal ($n = 2$); Diamond ($n = 3$); Fertilizer Elements – P, K ($n = 12$); Graphite ($n = 2$); Heavy Mineral Sands ($n = 1$); Iron Ore ($n = 5$); Other Metals – Sn, Sb, W, Ta, Nb ($n = 6$); Platinum Group Elements ($n = 2$); Precious Metals – Au, Ag ($n = 13$); Rare Earth Elements ($n = 6$); and Uranium ($n = 1$).

6 Data availability

The new spatial Sr isotope dataset for the northern Australia region is publicly available from https://doi.org/10.26186/147473 (de Caritat et al., 2022a) and via the Geoscience Australia portal https://portal.ga.gov.au/restore/cd686f2d-c87b-41b8-8c4b-ca8af531ae7e (last access: 27 February 2023; Geoscience Australia, 2023). Metadata are also available via the Geoscience Australia portal (https://portal.ga.gov.au/metadata/geochronology-and-isotopes/isotopes/rbsr-isotope-points/4cacd9e8-3340-4c27-99fe-48d404e67ca8, last access: 27 February 2023) (Geoscience Australia, 2022b).

7 Conclusions

A total of 372 new strontium (Sr) isotopic compositions ($^{87}Sr/^{86}Sr$) are reported from 357 catchment outlet sediment samples from northern Australia (north of 21.5° S). The analysed material originates from the sample archives of the National Geochemical Survey of Australia (NGSA; $n = 344$) and Northern Australia Geochemical Survey (NAGS; $n = 28$) projects, both of which targeted overbank or floodplain landforms near the outlet of large catchments. The sampled catchments together cover 1.536×10^6 km^2 of northern Australia. For the most part, bottom outlet sediment (BOS) samples, retrieved mostly by drilling (with an auger) to, on average, 0.6 to 0.8 m depth, were analysed. However, a few top outlet sediment (TOS) samples, collected from the top 0.1 m of soil, were also included, notably all of the NAGS samples and 18 NGSA samples. *Total* digestion of milled < 2 mm grain-size fractions from these sediments yielded a wide range of $^{87}Sr/^{86}Sr$ values from a minimum of 0.7048 to a maximum of 1.0330.

To date, the present study represents the largest Sr isoscape in the Southern Hemisphere, a region that is critically underrepresented in terms of isotopic data worldwide. We found a very strong correlation between the $^{87}Sr/^{86}Sr$ values in the BOS and TOS samples, allowing us to confidently infer BOS-equivalent values where only TOS samples were analysed. A map of the $^{87}Sr/^{86}Sr$ distribution (isoscape) across northern Australia reveals spatial patterns reflecting the ages and lithologies of the source material for the sediment, which is principally carried down catchment by fluvial processes. There is an overall increase in $^{87}Sr/^{86}Sr$ observed with increasing age of the geological region intersected at the sampling points. In areas of outcropping or sub-cropping felsic igneous rocks, relatively radiogenic Sr signatures are observed, whereas the inverse is noted for areas of mafic igneous rocks or marine sediments. The new Sr isotopic data are also examined in terms of the mineral occurrences found in their catchment. Whilst most mineral occurrences in the region are found in a catchment with an $^{87}Sr/^{86}Sr$ signature $\ll 0.84$, six outlier occurrences are associated with higher values. Some mineral occurrence types (Platinum Group Elements, Rare Earth Elements, Heavy Mineral Sands, and Diamond) are not found in catchments with $^{87}Sr/^{86}Sr$ signature less radiogenic than 0.75 in this study. Whether mineral system or regional petrogenetic processes are responsible for the association of relatively elevated $^{87}Sr/^{86}Sr$ with mineral deposits is a subject for further investigation.

Although we have focused the discussion of the new $^{87}Sr/^{86}Sr$ data on sediment sources in terms of rock ages and types, potential applications of the present isoscape and modelling derived therefrom could be extended to studies of

mineralization, hydrology, food tracing, dust provenancing or sourcing, and historic migrations of people and animals.

Supplement. The supplement related to this article is available online at: https://doi.org/10.5194/essd-15-1655-2023-supplement.

Author contributions. PdC provided the concept, samples, and funding, curated and analyzed the data, created the figures, and wrote and edited the manuscript. AD provided technical guidance, resources, and supervision, curated the data, and edited the manuscript. FD carried out the analyses, provided technical support, and curated the data.

Competing interests. The contact author has declared that none of the authors has any competing interests.

Disclaimer. This paper is published with the permission of the Chief Executive Officer, Geoscience Australia.

Publisher's note: Copernicus Publications remains neutral with regard to jurisdictional claims in published maps and institutional affiliations.

Acknowledgements. The National Geochemical Survey of Australia (NGSA) project would not have been possible without Commonwealth funding through the "Onshore Energy Security Program" (http://www.ga.gov.au/ngsa, last access: 27 February 2023), and Geoscience Australia appropriation. The Northern Australia Geochemical Survey (NAGS) project was funded under the "Exploring for the Future" programme (https://eftf-production.ga.gov.au/northern-australia-geochemical-survey, last access: 27 February 2023) and Geoscience Australia appropriation. Collaboration with the geoscience agencies of all states and the Northern Territory is gratefully recognized. We acknowledge all land owners and custodians, whether private, corporate, and/or traditional, for granting access to the field sites for the purposes of sampling. We are also grateful to Geoscience Australia laboratory staff for assistance with preparing and analysing the samples. We thank Geoscience Australia reviewers, Kathryn Waltenberg and David Huston; journal reviewers, Ian Moffat, Malte Willmes, and Jodie Pritchard; and the journal editor, Attila Demény, for their detailed and constructive critique of our work.

Financial support. This research has been supported by the Australian Government (Exploring for the Future, https://www.eftf.ga.gov.au/about, last access: 27 February 2023). Geoscience Australia's Exploring for the Future programme provides pre-competitive information to inform decision-making by government, community, and industry on the sustainable development of Australia's mineral, energy, and groundwater resources. By gathering, analysing, and interpreting new and existing pre-competitive geoscience data and knowledge, we are building a national picture of Australia's geology and resource potential. This leads to a strong economy, resilient society, and sustainable environment for the benefit of all Australians. This includes supporting Australia's transition to net-zero emissions; strong, sustainable resources and agriculture sectors; and economic opportunities and social benefits for Australia's regional and remote communities. The Exploring for the Future programme, which commenced in 2016, is an 8-year, AUD 225 million investment by the Australian Government.

Review statement. This paper was edited by Attila Demény and reviewed by Jodie Pritchard, Ian Moffat, and Malte Willmes.

References

Åberg, G.: The use of natural strontium isotopes as tracers in environmental studies, Wat. Air Soil Poll., 79, 309–322, https://doi.org/10.1007/BF01100444, 1995.

Åberg, G., Jacks, G., and Hamilton, P. J.: Weathering rates and $^{87}Sr/^{86}Sr$ ratios: an isotopic approach, J. Hydrol., 109, 65–78, https://doi.org/10.1016/0022-1694(89)90007-3, 1989.

Åberg, G., Wickman, T., and Mutvei, H.: Strontium isotope ratios in mussel shells as indicators of acidification, Ambio, 24, 265–268, 1995.

Adams, S., Grün, R., McGahan, D., Zhao, J.-X., Feng, Y., Nguyen, A., Willmes, M., Quaresimin, M., Lobsey, B., Collard, M., and Westaway, M. C.: A strontium isoscape of north-east Australia for human provenance and repatriation, Geoarchaeol., 34, 231–251, https://doi.org/10.1002/gea.21728, 2019.

Ahmad, M. and Scrimgeour, I. R.: Geological framework, chap. 2, in: Geology and Mineral Resources of the Northern Territory, edited by: Ahmad, M. and Munson, T. J., Northern Territory Geol. Surv., Special Publication, 5, 2:1–2:16, https://geoscience.nt.gov.au/gemis/ntgsjspui/bitstream/1/81482/1/GNT_Ch02_GeolFrame.pdf (last access: 27 February 2023), 2013.

Andersson, P., Lofvendahl, R., and Åberg, G.: Major element chemistry, δ^2H, $\delta^{18}O$ and $^{87}Sr/^{86}Sr$ in a snow profile across central Sweden, Atmos. Environ., 24A, 2601–2608, https://doi.org/10.1016/0960-1686(90)90138-D, 1990.

Andersson, P. S., Wasserburg, G. J., and Ingri, J.: The sources and transport of Sr and Nd isotopes in the Baltic Sea, Earth Planet. Sc. Lett., 113, 459–472, https://doi.org/10.1016/0012-821X(92)90124-E, 1992.

Andersson, P. S., Wasserburg, G. J., Ingri, J., and Stordal, M. C. Strontium, dissolved and particulate loads in fresh and brackish waters: the Baltic Sea and Mississippi Delta, Earth Planet. Sc. Lett., 124, 195–210, https://doi.org/10.1016/0012-821X(94)00062-X, 1994.

Australian Soil Resource Information System (ASRIS): Digital Atlas of Australian Soils, ASRIS [data set], https://www.asris.csiro.au/themes/Atlas.html (last access: 27 February 2023), 2022a.

Australian Soil Resource Information System (ASRIS): ASRIS Map Viewer Tool, Landcover Layer, Land Use 2001–2002, http://www.asris.csiro.au/mapping/viewer.htm (last access: 27 February 2023), 2022b.

Bagheri, R., Nadri, A., Raeisi, E., Eggenkamp, H. G. M., Kazemi, G. A., and Montaseri, A.: Hydrochemical and isotopic ($\delta^{18}O$,

δ^2H, $^{87}Sr/^{86}Sr$, δ^{37}Cl and δ^{81}Br) evidence for the origin of saline formation water in a gas reservoir, Chem. Geol., 384, 62–75, https://doi.org/10.1016/j.chemgeo.2014.06.017, 2014.

Bastrakov, E. N. and Main, P. T.: Northern Australia Geochemical Survey: a review of regional soil geochemical patterns, in: Exploring for the Future: Extended Abstracts, edited by: Czarnota, K., Roach, I., Abbott, S., Haynes, M., Kositcin, N., Ray, A., and Slatter, E., Geoscience Australia, Canberra, 1–4, https://doi.org/10.11636/134367, 2020.

Bataille, C. P. and Bowen, G. J.: Mapping $^{87}Sr/^{86}Sr$ variations in bedrock and water for large scale provenance studies, Chem. Geol., 304, 39–52, https://doi.org/10.1016/j.chemgeo.2012.01.028, 2012.

Bataille, C. P., Brennan, S. R., Hartmann, J., Moosdorf, N., Wooller, M. J., and Bowen, G. J.: A geostatistical framework for predicting variability in strontium concentrations and isotope ratios in Alaskan rivers, Chem. Geol., 389, 1–15, https://doi.org/10.1016/j.chemgeo.2014.08.030, 2014.

Bataille, C. P., von Holstein, I. C. C., Laffoon, J. E., Willmes, M., Liu, X.-M., and Davies, G. R.: A bioavailable strontium isoscape for Western Europe: a machine learning approach, PLoS ONE, 13, e0197386, https://doi.org/10.1371/journal.pone.0197386, 2018.

Bataille, C. P., Crowley, B. E., Wooller, M. J., and Bowen, G. J.: Advances in global bioavailable strontium isoscapes, Palaeogeogr. Palaeocl. Palaeoecol., 555, 109849, https://doi.org/10.1016/j.palaeo.2020.109849, 2020.

Bathgate, H., Lovett, A., Clarke, J., Ueckermann, H., and Hoogewerff, J.: The use of $^{87}Sr/^{86}Sr$ ratios, trace elements and biological profiling for forensic provenancing of soils, Eur. Geoph. Union Gen. Assembly 2011, 3–8 April 2011, Vienna, Austria, Geophys. Res. Abstr., 13, EGU2011-6592, 2011.

Bennett, R. and Gellatly, D. C.: Rb-Sr age determinations of some rocks from the West Kimberley Region, Western Australia, Bur. Min. Res. Geol. Geoph. Record, 1970/20, 14 pp., https://d28rz98at9flks.cloudfront.net/12433/Rec1970_020.pdf (last access: 27 February 2023), 1970.

Betts, P. G., Giles, D., Lister, G. S., and Frick, L. R.: Evolution of the Australian lithosphere, Austral. J. Earth Sci., 49, 661–695, https://doi.org/10.1046/j.1440-0952.2002.00948.x, 2002.

Black, L. P.: Tables of Isotopic Ages from the Georgetown Inlier, North Queensland, Bur. Min. Res. Geol. Geoph. Record, 1973/50, 2 pp., http://pid.geoscience.gov.au/dataset/ga/12874 (last access: 27 February 2023), 1973.

Black, L. P., Shaw, R. D., and Stewart, A. J.: Rb-Sr geochronology of Proterozoic events in the Arunta inlier, central Australia, Bur. Min. Res. J. Austral. Geol. Geoph., 8, 129–137, 1983.

Blake, D. H. and Kilgour, B.: Geological Regions of Australia 1 : 5 000 000 scale, Geosci. Austral., Canberra [data set], http://pid.geoscience.gov.au/dataset/ga/32366 (last access: 27 February 2023), 1998.

Blewett, R. (Ed.): Shaping a Nation – A Geology of Australia, Geosci. Austral. and ANU E Press, Canberra, https://doi.org/10.22459/SN.08.2012, 2012.

Blum, J. D. and Erel, Y.: A silicate weathering mechanism linking increases in marine $^{87}Sr/^{86}Sr$ with global glaciation, Nature, 373, 415–418, https://doi.org/10.1038/373415a0, 1995.

Blum, J. D., Erel, Y., and Brown, K.: $^{87}Sr/^{86}Sr$ ratios of Sierra Nevada stream waters: implications for relative mineral weathering rates, Geochim. Cosmochim. Ac., 57, 5019–5025, https://doi.org/10.1016/S0016-7037(05)80014-6, 1994.

Bolonin, A.: Oxygen and carbon isotope composition in primary carbonatites of the world: data summary and linear trends. Open J. Geol., 9, 424–439, https://doi.org/10.4236/ojg.2019.98028, 2019.

Braun, J., Dooley, J., Goleby, B., van der Hilst, R., and Klootwijk, C. (Eds.): Structure and Evolution of the Australian Plate, Am. Geoph. Union, Geodyn. Series, 26, ISBN 9780875905280, https://doi.org/10.1029/GD026, 1998.

Bullen, T., White, A., Blum, A., Harden, J., and Schulz, M.: Chemical weathering of a soil chronosequence on granitoid alluvium: II. Mineralogic and isotopic constraints on the behavior of strontium, Geochim. Cosmochim. Ac., 61, 291–306, https://doi.org/10.1016/S0016-7037(96)00344-4, 1997.

Bullen, T. D., Blum, A. E., White, A. F., and Schulz, M. S.: A model for the temporal evolution of $^{87}Sr/^{86}Sr$ of the cation exchange pool in a simple granitoid weathering system: approach and implications, Eos, 75, 280–281, 1994.

Bureau of Meteorology (BOM): Climate classification maps, http://www.bom.gov.au/jsp/ncc/climate_averages/climate-classifications/index.jsp?maptype=_tmp_zones#maps (last access: 27 February 2023), 2022a.

Bureau of Meteorology (BOM): Map of Climate Zones of Australia, http://www.bom.gov.au/climate/how/newproducts/images/zones.shtml (last access: 27 February 2023), 2022b.

Bureau of Meteorology (BOM): Decadal and multi-decadal temperature, http://www.bom.gov.au/jsp/ncc/climate_averages/decadal-temperature/index.jsp?maptype=1&period=9605 (last access: 27 February 2023), 2022c.

Bureau of Meteorology (BOM): Recent and historical rainfall maps, http://www.bom.gov.au/climate/maps/rainfall/?variable=rainfall&map=totals&period=48month&region=nat&year=2009&month=11&day=30 (last access: 27 February 2023), 2022d.

Cartwright, I., Weaver, T., and Petrides, B.: Controls on $^{87}Sr/^{86}Sr$ ratios of groundwater in silicate-dominated aquifers: SE Murray Basin, Australia, Chem. Geol., 246, 107–123, https://doi.org/10.1016/j.chemgeo.2007.09.006, 2007.

Chadwick, O. A., Derry, L. A., Bern, C. R., and Vitousek, P. M.: Changing sources of strontium to soils and ecosystems across the Hawaiian Islands, Chem. Geol., 267, 64–76, https://doi.org/10.1016/j.chemgeo.2009.01.009, 2009.

Christensen, J. N., Dafflon, B., Shiel, A. E., Tokunaga, T. K., Wan, J., Faybishenko, B., Dong, W., Williams, K. H., Hobson, C., Brown, S. T., and Hubbard, S. S.: Using strontium isotopes to evaluate the spatial variation of groundwater recharge, Sci. Total Environ., 637–638, 672–685, https://doi.org/10.1016/j.scitotenv.2018.05.019, 2018.

Collerson, K. D., Ullman, W. J., and Torgersen, T. Ground waters with unradiogenic $^{87}Sr/^{86}Sr$ ratios in the Great Artesian Basin, Australia, Geology, 16, 59–63, https://doi.org/10.1130/0091-7613(1988)016<0059:GWWUSS>2.3.CO;2, 1988.

Cooper, M., de Caritat, P., Burton, G., Fidler, R., Green, G., House, E., Strickland, C., Tang, J., and Wygralak, A.: National Geochemical Survey of Australia: Field Data, Record, 2010/18, Geosci. Austral., Canberra, https://doi.org/10.11636/Record.2011.020, 2010.

Daneshvar, N., Azizi, H., Asahara, Y., Tsuboi, M., and Hosseini, M.: Rare earth elements and Sr isotope ratios of large apatite crystals in Ghareh Bagh mica mine, NW Iran: tracing for petrogenesis and mineralization, Minerals, 10, 833, https://doi.org/10.3390/min10090833, 2020.

Dart, R. C., Barovich, K. M., Chittleborough, D. J., and Hill, S. M.: Calcium in regolith carbonates of central and southern Australia: its source and implications for the global carbon cycle, Palaeogeogr. Palaeocl. Palaeoecol., 249, 322–334, https://doi.org/10.1016/j.palaeo.2007.02.005, 2007.

de Almeida, B. S.: $^{87}Sr/^{86}Sr$ Isotopic Characterization as a Tool for the Designation of Origin and Geographical Indication: Application to Volcanic Rocks, Soils, Grapes and Wines from Brazil and Italy, Doctoral Thesis, University Frederic II of Naples, 106 pp., https://doi.org/10.13140/RG.2.2.15861.70882, 2021.

de Caritat, P.: The National Geochemical Survey of Australia: review and impact. Geochemistry: Exploration, Environment, Analysis, geochem2022-032, https://doi.org/10.1144/geochem2022-032, 2022.

de Caritat, P. and Cooper, M.: National Geochemical Survey of Australia: The Geochemical Atlas of Australia, Record, 2011/20, Geosci. Austral., Canberra, https://doi.org/10.11636/Record.2011.020, 2011a.

de Caritat, P. and Cooper, M.: National Geochemical Survey of Australia: Data Quality Assessment, Record, 2011/21, Geosci. Austral., Canberra, http://pid.geoscience.gov.au/dataset/ga/71971 (last access: 27 February 2023), 2011b.

de Caritat, P. and Cooper, M.: A continental-scale geochemical atlas for resource exploration and environmental management: the National Geochemical Survey of Australia, Geochem. Explo. Env. Anal., 16, 3–13, https://doi.org/10.1144/geochem2014-322, 2016.

de Caritat, P., Kirste, D., Carr, G., and McCulloch, M.: Groundwater in the Broken Hill region, Australia: recognising interaction with bedrock and mineralisation using S, Sr and Pb isotopes, Appl. Geochem., 20, 767–787, https://doi.org/10.1016/j.apgeochem.2004.11.003, 2005.

de Caritat, P., Cooper, M., Lech, M., McPherson, A., and Thun, C.: National Geochemical Survey of Australia: Sample Preparation Manual, Record, 2009/08, Geosci. Austral., Canberra, http://pid.geoscience.gov.au/dataset/ga/68657 (last access: 27 February 2023), 2009.

de Caritat, P., Cooper, M., Pappas, W., Thun, C., and Webber, E.: National Geochemical Survey of Australia: Analytical Methods Manual, Record, 2010/15, Geosci. Austral., Canberra, http://pid.geoscience.gov.au/dataset/ga/70369 (last access: 27 February 2023), 2010.

de Caritat, P., Dosseto, A., and Dux, F.: A strontium isoscape of northern Australia, Geosci. Austral., Canberra [data set], https://doi.org/10.26186/147473, 2022a.

de Caritat, P., Dosseto, A., and Dux, F.: A strontium isoscape of inland southeastern Australia, Earth Syst. Sci. Data, 14, 4271–4286, https://doi.org/10.5194/essd-14-4271-2022, 2022b.

De Deckker, P.: OZ-3 northern Western Australia sampling trip and analysis: strontium, rubidium and neodymium isotopes, Pangaea [data set], https://doi.org/10.1594/PANGAEA.907689, 2019.

De Deckker, P.: Airborne dust traffic from Australia in modern and Late Quaternary times, Global Planet. Change, 184, 103056, https://doi.org/10.1016/j.gloplacha.2019.103056, 2020.

De Deckker, P., Munday, C. I., Brocks, J., O'loingsigh, T., Allison, G. E., Hope, J., Norman, M., Stuut, J.-B. W., Tapper, N. J., and van der Kaars, S.: Characterisation of the major dust storm that traversed over eastern Australia in September 2009; a multidisciplinary approach, Aeol. Res., 15, 133–149, https://doi.org/10.1016/j.aeolia.2014.07.003, 2014.

Denison, R. E., Koepnick, R. B., Burke, W. H., Hetherington, E. A., and Fletcher, A.: Construction of the Mississippian, Pennsylvanian and Permian seawater $^{87}Sr/^{86}Sr$ curve, Chem. Geol., 112, 145–167, https://doi.org/10.1016/0009-2541(94)90111-2, 1994a.

Denison, R. E., Koepnick, R. B., Fletcher, A., Howell, M. W., and Callaway, W. S.: Criteria for the retention of original seawater $^{87}Sr/^{86}Sr$ in ancient shelf limestones, Chem. Geol., 112, 131–143, https://doi.org/10.1016/0009-2541(94)90110-4, 1994b.

Department of Industry, Science, Energy and Resources (DISER): 2022 Critical Minerals Strategy, Aust. Gov., Canberra, https://www.industry.gov.au/publications/critical-minerals-strategy-2022, last access: 27 February 2023, 2022.

Di Paola-Naranjo, R. D., Baroni, M. V., Podio, N. S., Rubinstein, H. R., Fabani, M. P., Badini, R. G., Inga, M., Ostera, H. A., Cagnoni, M., Gallegos, E., Gautier, E., Peral-Garcia, P., Hoogewerff, J., and Wunderlin, D. A.: Fingerprints for main varieties of Argentinean wines: terroir differentiation by inorganic, organic, and stable isotopic analyses coupled to chemometrics, J. Ag. Food Chem., 59, 7854–7865, https://doi.org/10.1021/jf2007419, 2011.

Dogramaci, S. S. and Herczeg, A. L.: Strontium and carbon isotope constraints on carbonate-solution interactions and inter-aquifer mixing in groundwaters of the semi-arid Murray Basin, Australia, J. Hydrol., 262, 50–67, https://doi.org/10.1016/S0022-1694(02)00021-5, 2002.

Douglas, G. B., Gray, C. M., Hart, B. T., and Beckett, R.: A strontium isotopic investigation of the origin of suspended particulate matter (SPM) in the Murray-Darling River system, Australia, Geochim. Cosmochim. Ac., 59, 3799–3815, https://doi.org/10.1016/0016-7037(95)00266-3, 1995.

Evans, J. A., Montgomery, J., Wildman, G., and Boulton, N.: Spatial variations in biosphere $^{87}Sr/^{86}Sr$ in Britain, J. Geol. Soc., 167, 1–4, https://doi.org/10.1144/0016-76492009-090, 2010.

Faure, G. and Felder, R. P.: Isotopic composition of strontium and sulfur in secondary gypsum crystals, Brown Hills, Transantarctic Mountains, J. Geoch. Explo., 14, 265–270, https://doi.org/10.1016/0375-6742(81)90116-3, 1981.

Flecker, R., de Villiers, S., and Ellam, R. M.: Modelling the effect of evaporation on the salinity-$^{87}Sr/^{86}Sr$ relationship in modern and ancient marginal-marine systems: the Mediterranean Messinian Salinity Crisis, Earth Planet. Sc. Lett., 203, 221–233, https://doi.org/10.1016/S0012-821X(02)00848-8, 2002.

Frei, R. and Frei, K. M.: The geographic distribution of Sr isotopes from surface waters and soil extracts over the island of Bornholm (Denmark) – A base for provenance studies in archeology and agriculture, Appl. Geochem., 38, 147–160, https://doi.org/10.1016/j.apgeochem.2013.09.007, 2013.

Geoscience Australia (GA): Australia's River Basins 1997 – Product User Guide, Geosci. Austral., Canberra, http://pid.geoscience.gov.au/dataset/ga/42343 (last access: 27 February 2023), 1997.

Geoscience Australia (GA): 9 Second Digital Elevation Model of Australia Version 3, Geosci. Austral., Canberra [data set], http://pid.geoscience.gov.au/dataset/ga/89580 (last access: 27 February 2023), 2008.

Geoscience Australia (GA): Australian Operating Mines Map 2021 Data, Geosci. Austral., Canberra [data set], https://doi.org/10.26186/147010 (last access: 27 February 2023), 2022a.

Geoscience Australia: Geoscience Australia Portal: Geochronology and Isotopes – Isotopes – Rb-Sr Isotope – Points, Australian Government [data set], https://portal.ga.gov.au/metadata/geochronology-and-isotopes/isotopes/rbsr-isotope-points/4cacd9e8-3340-4c27-99fe-48d404e67ca8 (last access: 27 February 2023), 2022b.

Geoscience Australia: Geochronology and Isotopes Data Portal, https://portal.ga.gov.au/restore/cd686f2d-c87b-41b8-8c4b-ca8af531ae7e, Geoscience Australia [data set], last access: 27 February 2023.

Gingele, F. X. and De Deckker, P.: Clay mineral, geochemical and Sr-Nd-isotopic fingerprinting of sediments in the Murray-Darling fluvial system, southeast Australia, Aust. J. Earth Sci., 52, 965–974, https://doi.org/10.1080/08120090500302301, 2005.

Gosselin, D. C., Harvey, F. E., Frost, C., Stotler, R., and Macfarlane, P. A.: Strontium isotope geochemistry of groundwater in the central part of the Dakota (Great Plains) aquifer, USA, Appl. Geochem., 19, 359–377, https://doi.org/10.1016/S0883-2927(03)00132-X, 2004.

Gosz, J. R., Brookins, D. G., and Moore, D. I.: Using strontium isotope ratios to estimate inputs to ecosystems, Bioscience, 33, 23–30, https://doi.org/10.2307/1309240, 1983.

Graustein, W. C.: $^{87}Sr/^{86}Sr$ ratios measure the sources and flow of strontium in terrestrial ecosystems, chap. 28, in: Stable Isotopes in Ecological Research, edited by: Rundel, P. W., Ehleringer, J. R., and Nagy, K. A., Springer-Verlag, New York, 491–512, https://doi.org/10.1007/978-1-4612-3498-2_28, 1989.

Green, G. P., Bestland, E. A., and Walker, G. S.: Distinguishing sources of base cations in irrigated and natural soils: evidence from strontium isotopes, Biogeochem., 68, 199–225, https://doi.org/10.1023/B:BIOG.0000025743.34079.d3, 2004.

Griffin, T. J., Page, R., Sheppard, S., and Tyler, I.: Tectonic implications of Palaeoproterozoic post-collisional, high-K felsic igneous rocks from the Kimberley region of northwestern Australia, Precambrian Res., 101, 1–23, https://doi.org/10.1016/S0301-9268(99)00084-4, 2000.

Grobe, M., Machel, H. G., and Heuser, H.: Origin and evolution of saline groundwater in the Münsterland Cretaceous Basin, Germany: oxygen, hydrogen, and strontium isotope evidence, J. Geoch. Explo., 69–70, 5–9, https://doi.org/10.1016/S0375-6742(00)00009-1, 2000.

Gruszczynski, M., Hoffman, A., Krzysztof, M., and Veizer, J.: Seawater strontium isotopic perturbation at the Permian-Triassic boundary, west Spitsbergen, and its implications for the interpretation of strontium isotopic data, Geology, 20, 779–782, https://doi.org/10.1130/0091-7613(1992)020<0779:SSIPAT>2.3.CO;2, 1992.

Hagedorn, B., Cartwright, I., Raveggi, M., and Maas, R.: Rare earth element and strontium geochemistry of the Australian Victorian Alps drainage system: Evaluating the dominance of carbonate vs. aluminosilicate weathering under varying runoff, Chem. Geol., 284, 105–126, https://doi.org/10.1016/j.chemgeo.2011.02.013, 2011.

Harrington, G. A. and Herczeg, A. L.: The importance of silicate weathering of a sedimentary aquifer in arid Central Australia indicated by very high $^{87}Sr/^{86}Sr$ ratios, Chem. Geol., 199, 281–292, https://doi.org/10.1016/S0009-2541(03)00128-1, 2003.

Hoogewerff, J. A., Reimann, C., Ueckermann, H., Frei, R., Frei, K. M., van Aswegen, T., Stirling, C., Reid, M., Clayton, A., Ladenberger, A., and The GEMAS Project Team: Bioavailable $^{87}Sr/^{86}Sr$ in European soils: a baseline for provenancing studies, Sci. Total Environ., 672, 1033–1044, https://doi.org/10.1016/j.scitotenv.2019.03.387, 2019.

Huston, D. L., Maas, R., Cross, A., Hussey, K. J., Mernagh, T. P., Fraser, G., and Champion, D. C.: The Nolans Bore rare-earth element-phosphorus-uranium mineral system: geology, origin and post-depositional modifications, Miner. Deposita, 51, 797–822, https://doi.org/10.1007/s00126-015-0631-y, 2016.

Huston, D. L., Champion, D. C., Czarnota, K., Duan, J., Hutchens, M., Paradis, S., Hoggard, M., Ware, B., Gibson, G. M., Doublier, M. P., Kelley, K., McCafferty, A., Hayward, N., Richards, F., Tessalina, S., and Carr, G.: Zinc on the edge–isotopic and geophysical evidence that cratonic edges control world-class shale-hosted zinc-lead deposits, Miner. Deposita, 58, 707–729, https://doi.org/10.1007/s00126-022-01153-9, 2022.

Isbell, R. F. and National Committee on Soil and Terrain: The Australian Soil Classification, third edn., CSIRO Publishing, Melbourne, Victoria, 181 pp., https://ebooks.publish.csiro.au/content/australian-soil-classification-9781486314782 (last access: 27 February 2023), 2021.

Jacks, G., Åberg, G., and Hamilton, P. J.: Calcium budgets for catchments as interpreted by strontium isotopes, Hydrol. Res., 20, 85–96, https://doi.org/10.2166/nh.1989.0007, 1989.

Jomori, Y., Minami, M., Sakurai-Goto, A., and Ohta, A.: Comparing the $^{87}Sr/^{86}Sr$ of the bulk and exchangeable fractions in stream sediments: implications for $^{87}Sr/^{86}Sr$ mapping in provenance studies, Appl. Geochem., 86, 70–83, https://doi.org/10.1016/j.apgeochem.2017.09.004, 2017.

Jweda, J., Bolge, L., Class, C., and Goldstein, S. L.: High precision Sr-Nd-Hf-Pb isotopic compositions of USGS reference material BCR-2, Geostand. Geoanal. Res., 40, 101–115, https://doi.org/10.1111/j.1751-908X.2015.00342.x, 2016.

Kennedy, M. J., Hedin, L. O., and Derry, L. A.: Decoupling of unpolluted temperate forests from rock nutrient sources revealed by natural $^{87}Sr/^{86}Sr$ and ^{84}Sr tracer addition, P. Nat. Acad. Sci. USA, 99, 9639–9644, https://doi.org/10.1073/pnas.152045499, 2002.

Knudson, K. J., Webb, E., White, C., and Longstaffe, F. J.: Baseline data for Andean paleomobility research: a radiogenic strontium isotope study of modern Peruvian agricultural soils, Archaeol. Anthropol. Sci., 6, 205–219, https://doi.org/10.1007/s12520-013-0148-1, 2014.

Le Bas, M., Spiro, B., and Yang, X.: Oxygen, carbon and strontium isotope study of the carbonatitic dolomite host of the Bayan Obo Fe-Nb-REE deposit, Inner Mongolia, N China, Mineral. Mag., 61, 531–541, https://doi.org/10.1180/minmag.1997.061.407.05, 1997.

Lech, M. E., de Caritat, P., and Mcpherson, A. A.: National Geochemical Survey of Australia: Field Manual, Record, 2007/08,

Geosci. Austral., Canberra, http://pid.geoscience.gov.au/dataset/ga/65234 (last access: 27 February 2023), 2007.

Lugli, F., Cipriani, A., Bruno, L., Ronchetti, F., Cavazzuti, C., and Benazzi, S.: A strontium isoscape of Italy for provenance studies, Chem. Geol., 587, 120624, https://doi.org/10.1016/j.chemgeo.2021.120624, 2022.

Lyons, W. B., Tyler, S. W., Gaudette, H. E., and Long, D. T.: The use of strontium isotopes in determining groundwater mixing and brine fingering in a playa spring zone, Lake Tyrrell, Australia, J. Hydrol., 167, 225–239, https://doi.org/10.1016/0022-1694(94)02601-7, 1995.

McArthur, J. M., Howarth, R. J., and Shields, G. A.: Strontium Isotope Stratigraphy, Chap. 7 in: The Geologic Time Scale, edited by: F. M., Ogg, J. G., Schmitz, M., and Ogg, G., Elsevier BV, 127–144, https://doi.org/10.1016/B978-0-12-824360-2.00007-3, 2012.

McNutt, R. H.: Strontium Isotopes, in: Environmental Tracers in Subsurface Hydrology, edited by: Cook P. G. and Herczeg A. L., Springer, Boston, MA, https://doi.org/10.1007/978-1-4615-4557-6_8, 2000.

McNutt, R. H., Frape, S. K., and Dollar, P.: A strontium, oxygen and hydrogen isotopic composition of brines, Michigan and Appalachian Basins, Ontario and Michigan, Appl. Geochem., 2, 495–505, https://doi.org/10.1016/0883-2927(87)90004-7, 1987.

Moffat, I., Rudd, R., Willmes, M., Mortimer, G., Kinsley, L., McMorrow, L., Armstrong, R., Aubert, M., and Grün, R.: Bioavailable soil and rock strontium isotope data from Israel, Earth Syst. Sci. Data, 12, 3641–3652, https://doi.org/10.5194/essd-12-3641-2020, 2020.

Mountjoy, E. W., Qing, H., and McNutt, R. H.: Strontium isotopic composition of Devonian dolomites, Western Canada Sedimentary Basin: significance of sources of dolomitizing fluids, Appl. Geochem., 7, 59–75, 1992.

Nebel, O. and Stammeier, J. A.: Strontium Isotopes, in: Encycl. Geochem., Encycl. Earth Sci. Series, edited by: White W. M., Springer, Cham, https://doi.org/10.1007/978-3-319-39312-4_137, 2018.

Négrel, P. and Grosbois, C.: Changes in chemical and $^{87}Sr/^{86}Sr$ signature distribution patterns of suspended matter and bed sediments in the upper Loire river basin (France), Chem. Geol., 156, 231–249, https://doi.org/10.1016/S0009-2541(98)00182-X, 1999.

Négrel, P. and Pauwels, H.: Interaction between different groundwaters in Brittany catchments (France): characterizing multiple sources through strontium- and sulphur isotope tracing, Wat. Air Soil Poll., 151, 261–285, https://doi.org/10.1023/B:WATE.0000009912.04798.b7, 2004.

Oishi, Y.: Is the Sr isotope ratio of mosses a good indicator for Asian dust (Kosa)?, Landscape Ecol. Eng., 18, 11–17, https://doi.org/10.1007/s11355-021-00476-5, 2021.

Ojiambo, S. B., Lyons, W. B., Welch, K. A., Poreda, R. J., and Johannesson, K. H.: Strontium isotopes and rare earth elements as tracers of groundwater-lake water interactions, Lake Naivasha, Kenya, Appl. Geochem., 18, 1789–1805, https://doi.org/10.1016/S0883-2927(03)00104-5, 2003.

Oliver, L., Harris, N., Bickle, M., Chapman, H., Dise, N., and Horstwood, M.: Silicate weathering rates decoupled from the $^{87}Sr/^{86}Sr$ ratio of the dissolved load during Himalayan erosion, Chem. Geol., 201, 119–139, https://doi.org/10.1016/S0009-2541(03)00236-5, 2003.

Ollier, C. D.: The regolith in Australia, Earth-Sci. Rev., 25, 355–361, https://doi.org/10.1016/0012-8252(88)90003-7, 1988.

Pacheco-Forés, S. I., Gordon, G. W., and Knudson, K. J.: Expanding radiogenic strontium isotope baseline data for central Mexican paleomobility studies, PLoS ONE, 15, e0229687, https://doi.org/10.1371/journal.pone.0229687, 2020.

Page, R. W., Needham, R. S., and Compston, W.: Geochronology and evolution of the Late-Archaean basement and Proterozoic rocks in the Alligator Rivers uranium field, Northern Territory, Australia, in: Proc. Int. Uranium Symp., Pine Creek Geosyncline (Sydney, New South Wales, 4–8 June 1979), edited by: Ferguson, J. and Goleby, A. B., Int. Atom. En. Agency, Vienna, Austria, 39–68, https://inis.iaea.org/collection/NCLCollectionStore/_Public/12/629/12629252.pdf, last access: 27 February 2023, 1980.

Pain, C., Gregory, L., Wilson, P., and McKenzie, N.: The Physiographic Regions of Australia – Explanatory Notes, Australian Collaborative Land Evaluation Program (ACLEP) and National Committee on Soil and Terrain (NCST), Canberra, 30 pp., https://publications.csiro.au/rpr/pub?pid=csiro%3AEP113843 (last access: 27 February 2023), 2011.

Palmer, M. R., Helvaci, C., and Fallick, A. E.: Sulphur, sulphate oxygen and strontium isotope composition of Cenozoic Turkish evaporates, Chem. Geol., 209, 341–356, https://doi.org/10.1016/j.chemgeo.2004.06.027, 2004.

Plumlee, G.: Basalt, Columbia River, BCR-2, Prelim. U.S. Geol. Surv. Cert. Anal., https://cpb-us-w2.wpmucdn.com/muse.union.edu/dist/c/690/files/2021/07/usgs-bcr2-1.pdf (last access: 27 February 2023), 1998.

Price, G. J., Ferguson, K. J., Webb, G. E., Feng, Y. X., Higgins, P., Nguyen, A. D., Zhao, J. X., Joannes-Boyau, R., and Louys, J.: Seasonal migration of marsupial megafauna in Pleistocene Sahul (Australia-New Guinea), P. Roy. Soc. B-Biol. Sci., 284, 20170785, https://doi.org/10.1098/rspb.2017.0785, 2017.

Probst, A., El Gh'Mari, A., Aubert, D., Fritz, B., and McNutt, R.: Strontium as a tracer of weathering processes in a silicate catchment polluted by acid atmospheric inputs, Strengbach, France, Chem. Geol., 170, 203–219, https://doi.org/10.1016/S0009-2541(99)00248-X, 2000.

Quade, J., Chivas, A. R., and McCulloch, M. T.: Strontium and carbon isotope tracers and the origins of soil carbonate in South Australia and Victoria, Palaeogeogr. Palaeocl. Palaeoecol., 113, 103–117, https://doi.org/10.1016/0031-0182(95)00065-T, 1995.

Raymond, O. L., Gallagher, R., Shaw, R., Yeates, A. N., Doutch, H. F., Palfreyman, W. D., Blake, D. H., and Highet, L.: Surface Geology of Australia 1 : 2.5 million scale dataset 2012 edition, edited by: Raymond, O. L. and Gallagher, R., Geosci. Austral., Canberra [data set], https://doi.org/10.26186/5c636e559cbe1, 2012.

Revel-Rolland, M., De Deckker, P., Delmonte, B., Hesse, P. P., Magee, J. W., Basile-Doelsch, I., Grousset, F., and Bosch, D.: Eastern Australia: a possible source of dust in East Antarctica interglacial ice, Earth Planet. Sc. Lett., 249, 1–13, https://doi.org/10.1016/j.epsl.2006.06.028, 2006.

Riley, G. H.: Granite ages in the Pine Creek Geosyncline, in: Proc. Int. Uranium Symp., Pine Creek Geosyncline, 4–8 June 1979, Sydney, New South Wales, edited by: Ferguson, J. and Goleby, A. B., Int. Atom. En. Agency, Vienna, Austria, 69–

72, https://inis.iaea.org/collection/NCLCollectionStore/_Public/12/629/12629252.pdf, last access: 27 February 2023, 1980.

Romaniello, S. J., Field, M. P., Smith, H. B., Gordon, G. W., Kim, M. H., and Anbar, A. D.: Fully automated chromatographic purification of Sr and Ca for isotopic analysis, J. Anal. Atomic Spectro., 30, 1906–1912, https://doi.org/10.1039/C5JA00205B, 2015.

Rotenberg, E., Davis, D. W., Amelin, Y., Ghosh, S., and Bergquist, B. A.: Determination of the decay-constant of ^{87}Rb by laboratory accumulation of ^{87}Sr, Geochim. Cosmochim. Ac., 85, 41–57, https://doi.org/10.1016/j.gca.2012.01.016, 2012.

Rundberg, Y. and Smalley, P. C.: High-resolution dating of Cenozoic sediments from northern North Sea using ^{87}Sr/^{86}Sr stratigraphy, Am. Assoc. Petrol. Geol. Bull., 73, 298–308, https://doi.org/10.1306/703C9B77-1707-11D7-8645000102C1865D, 1989.

Schaltegger, U., Stille, P., Rais, N., Pique, A., and Clauer, N.: Neodymium and strontium isotopic dating of diagenesis and low-grade metamorphism of argillaceous sediments, Geochim. Cosmochim. Ac., 58, 1471–1481, https://doi.org/10.1016/0016-7037(94)90550-9, 1994.

Schoneveld, L., Spandler, C., and Hussey, K.: Genesis of the central zone of the Nolans Bore rare earth element deposit, Northern Territory, Australia, Contrib. Mineral. Petrol., 170, 11, https://doi.org/10.1007/s00410-015-1168-x, 2015.

Schultz, J. L., Boles, J. R., and Tilton, G. R.: Tracking calcium in the San Joaquin basin, California: a strontium isotopic study of carbonate cements at North Coles Levee, Geochim. Cosmochim. Ac., 53, 1991–1999, https://doi.org/10.1016/0016-7037(89)90319-0, 1989.

Shewan, L. G., Armstrong, R. A., and O'Reilly, D.: Baseline bioavailable strontium isotope values for the investigation of residential mobility and resource-acquisition strategies in prehistoric Cambodia, Archaeom., 62, 810–826, https://doi.org/10.1111/arcm.12557, 2020.

Shields, G. A.: A normalised seawater strontium isotope curve and the Neoproterozoic-Cambrian chemical weathering event, eEarth Discuss., 2, 69–84, 2007.

Shin, W.-J., Ryu, J.-S., Kim, R.-H., and Min, J.-S.: First strontium isotope map of groundwater in South Korea: applications for identifying the geographical origin, Geosci. J., 25, 173–181, https://doi.org/10.1007/s12303-020-0013-z, 2021.

Simandl, G. J. and Paradis, S.: Vanadium as a critical material: economic geology with emphasis on market and the main deposit types, Appl. Earth Sci., 131, 218–236, https://doi.org/10.1080/25726838.2022.2102883, 2022.

Smalley, P. C., Råheim, A., Rundberg, Y., and Johansen, H.: Strontium-isotope stratigraphy: applications in basin modelling and reservoir correlation, chap. 3, in: Correlation in Hydrocarbon Exploration, Norwegian Petrol. Soc., Graham and Trotman, 23–31, https://doi.org/10.1007/978-94-009-1149-9_3, 1989.

Smalley, P. C., Lønøy, A., and Råheim, A.: Spatial ^{87}Sr/^{86}Sr variations in formation water and calcite from the Ekofisk chalk oil field: implications for reservoir connectivity and fluid composition, Appl. Geochem., 7, 341–350, https://doi.org/10.1016/0883-2927(92)90024-W, 1992.

Stueber, A. M., Pushkar, P., and Hetherington, E. A.: A strontium isotopic study of formation waters from the Illinois basin, USA, Appl. Geochem., 2, 477–494, https://doi.org/10.1016/0883-2927(87)90003-5, 1987.

Sullivan, M. D., Haszeldine, R. S., and Fallick, A. E.: Linear coupling of carbon and strontium isotopes in Rotliegend Sandstone, North Sea: evidence for cross-formational fluid flow, Geology, 18, 1215–1218, https://doi.org/10.1130/0091-7613(1990)018<1215:LCOCAS>2.3.CO;2, 1990.

Swart, P. K., Ruiz, J., and Holmes, C. W.: Use of strontium isotopes to constrain the timing and mode of dolomitization of upper Cenozoic sediments in a core from San Salvador, Bahamas, Geology, 15, 262–265, https://doi.org/10.1130/0091-7613(1987)15<262:UOSITC>2.0.CO;2, 1987.

Tukey, J. W.: Exploratory Data Analysis, Addison-Wesley Publishing Company, Reading, MA, 506 pp., 1977.

Van Kranendonk, M. J., Hickman, A. H., Smithies, R. H., Nelson, D. R., and Pike, G.: Geology and tectonic evolution of the Archean North Pilbara Terrain, Pilbara Craton, Western Australia, Econ. Geol., 97, 695–732, https://doi.org/10.2113/gsecongeo.97.4.695, 2002.

Veizer, J.: Strontium isotopes in seawater trough time, Ann. Rev. Earth Planet. Sci., 17, 141–167, https://doi.org/10.1146/annurev.ea.17.050189.001041, 1989.

Vinciguerra, V., Stevenson, R., Pedneault, K., Poirer, A., Hélie, J.-F., and Widory, D.: Strontium isotope characterization of Wines from the Quebec (Canada) Terroir, Proc. Earth Planet. Sci., 13, 252–255, https://doi.org/10.1016/j.proeps.2015.07.059, 2015.

Voerkelius, S., Lorenz, G. D., Rummel, S., Quétel, C. R., Heiss, G., Baxter, M., Brach-Papa, C., Deters-Itzelsberger, P., Hoelzl, S., Hoogewerff, J., Ponzevera, E., Bocxstaele, M., and Van Ueckermann, H.: Strontium isotopic signatures of natural mineral waters, the reference to a simple geological map and its potential for authentication of food, Food Chem., 118, 933–940, https://doi.org/10.1016/j.foodchem.2009.04.125, 2010.

Vorster, C., Greeff, L., and Coetzee, P. P.: The determination of ^{11}B/^{10}B and ^{87}Sr/^{86}Sr isotope ratios by quadrupole-based ICP-MS for the fingerprinting of South African wine, South Afric. J. Chem., 63, 207–214, 2010.

Washburn, E., Nesbitt, J., Ibarra, B., Fehren-Schmitz, L., and Oelze, V. M.: A strontium isoscape for the Conchucos region of highland Peru and its application to Andean archaeology, PLOS ONE 16, e0248209, https://doi.org/10.1371/journal.pone.0248209, 2021.

Wei, C.-W., Xu, C., Chakhmouradian, A. R., Brenna, M., Kynicky, J., and Song, W.-L.: Carbon-strontium isotope decoupling in carbonatites from Caotan (Qinling, China): implications for the origin of calcite carbonatite in orogenic settings, J. Petrol., 61, egaa024, https://doi.org/10.1093/petrology/egaa024, 2020.

Wei, X., Wang, S., Ji, H., and Shi, Z.: Strontium isotopes reveal weathering processes in lateritic covers in southern China with implications for paleogeographic reconstructions, PLOS ONE, 13, e0191780, https://doi.org/10.1371/journal.pone.0191780, 2018.

Wickman, T. and Jacks, G.: Strontium isotopes in weathering budgeting. In: Water-Rock Interaction, Proc. 7th Int. Symp. Water-Rock Interaction, 13–18 July 1992, Park City, Utah, edited by: Kharaka, Y. K. and Maest, A. S., Balkema, Rotterdam, 1, 611–614, ISBN 9054100753, 1992.

Wilford, J.: A weathering intensity index for the Australian continent using airborne gamma-ray spectrometry and

digital terrain analysis, Geoderma, 183–184, 124–142, https://doi.org/10.1016/j.geoderma.2010.12.022, 2012.

Willmes, M., McMorrow, L., Kinsley, L., Armstrong, R., Aubert, M., Eggins, S., Falguères, C., Maureille, B., Moffat, I., and Grün, R.: The IRHUM (Isotopic Reconstruction of Human Migration) database – bioavailable strontium isotope ratios for geochemical fingerprinting in France, Earth Syst. Sci. Data, 6, 117–122, https://doi.org/10.5194/essd-6-117-2014, 2014.

Willmes, M., Bataille, C. P., James, H. F., Moffat, I., McMorrow, L., Kinsley, L., Armstrong, R. A., Eggins, S., and Grün, R.: Mapping of bioavailable strontium isotope ratios in France for archaeological provenance studies, Appl. Geochem., 90, 75–86, https://doi.org/10.1016/j.apgeochem.2017.12.025, 2018.

Withnall, I. W., Hutton, L. J., Armit, R. J., Betts, P. G., Blewett, R. S., Champion, D. C., and Jell, P. A.: North Australian Craton. In: Geology of Queensland, edited by: Jell, P. A., Geol. Surv. Queensland, Brisbane, 23–112, ISBN 9781921489761, https://www.business.qld.gov.au/industries/mining-energy-water/resources/geoscience-information/reports-news/geology-queensland-book-map (last access: 27 February 2023), 2013.

Wyborn, L. A. I., Heinrich, C. A., and Jaques, A. L.: Australian Proterozoic mineral systems: essential ingredients and mappable criteria, Austral. Inst. Mining Metall. (AusIMM) Ann. Conf. Proc., 5–9 August 1994, Darwin, Northern Territory, 109–115, https://ecat.ga.gov.au/geonetwork/srv/api/records/a05f7892-f8a0-7506-e044-00144fdd4fa6 (last access: 27 February 2023), 1994.

Yang, C., Telmer, K., and Veizer, J.: Chemical dynamics of the "St. Lawrence" riverine system: δD_{H_2O}, $\delta^{18}O_{H_2O}$, $\delta^{13}C_{DIC}$, $\delta^{34}S_{sulfate}$, and dissolved $^{87}Sr/^{86}Sr$, Geochim. Cosmochim. Ac., 60, 851–866, https://doi.org/10.1016/0016-7037(95)00445-9, 1996.

Zhao, Z., Leach, D. L., Wei, J., Liang, S., and Pfaff, K.: Origin of the Xitieshan Pb-Zn deposit, Qinghai, China: evidence from petrography and S-C-O-Sr isotope geochemistry, Ore Geol. Rev., 139A, 104429, https://doi.org/10.1016/j.oregeorev.2021.104429, 2021.